Causes of the extensive hypoxia in the Gulf of Riga in 2018

Stella-Theresa Stoicescu[1], Jaan Laanemets[1], Taavi Liblik[1], Maris Skudra[2], Oliver Samlas[1], Inga Lips[1,3], Urmas Lips[1]

[1]Department of Marine Systems, Tallinn University of Technology, Tallinn, 19086, Estonia
[2]Latvian Institute of Aquatic Ecology, Riga, LV-1007, Latvia
[3]EuroGOOS AISBL, Brussels, 1000, Belgium

Correspondence to: Stella-Theresa Stoicescu (stella.stoicescu@taltech.ee)

Abstract. The Gulf of Riga is a relatively shallow bay connected to the deeper central Baltic Sea (Baltic Proper) via straits with sills. The decrease in the near-bottom oxygen levels from spring to autumn is a common feature in the gulf, but in 2018, extensive hypoxia was ~~exceptional~~observed. We analyzed temperature, salinity, oxygen, and nutrient data collected in 2018 ~~and~~, along with historical data available from environmental databases. ~~Forcing~~Meteorological and hydrological data from the study year were compared with their long-term means and variability. ~~The year~~ We suggest that pronounced oxygen depletion occurred in 2018 ~~was exceptional~~ due to ~~occasionally dominating~~a distinct development of vertical stratification. Seasonal stratification developed early and was stronger in spring-summer 2018 than on average due to high heat flux and weak winds. Dominating north-easterly winds ~~supporting~~in early spring and summer supported the inflow of saltier waters from the Baltic Proper ~~and meteorological conditions causing fast development of thermal stratification in spring. Existing stratification hindered~~that created an additional deep pycnocline restricting vertical transport between the near-bottom layer (NBL) and the water ~~layers~~column above ~~it~~. The estimated oxygen consumption rate at the sediment surface in spring-summer 2018 was about 1.7 mmol O_2 m^{-2} h^{-1} ~~that~~, which exceeded the oxygen input to the NBL due to advection and mixing. ~~We suggest that the observed pronounced oxygen depletion was magnified by the prolonged stratified season and haline stratification~~Such consumption rate leads to near-bottom hypoxia in ~~the deep layer that maintained a decreased water volume between~~all years when vertical mixing in autumn reaches the seabed ~~and the pycnocline~~later than on average according to the long-term (1979-2018) meteorological conditions. The observed increase in phosphate concentrations in the NBL in summer 2018 suggests a significant sediment phosphorus release in hypoxic conditions counteracting the mitigation measures to combat eutrophication. ~~We conclude, if similar~~Since climate change projections predict that meteorological conditions ~~as~~comparable to those in 2018 ~~could~~will occur more frequently in the future, ~~such~~ extensive hypoxia would be more common in the Gulf of Riga and other coastal basins with similar morphology and human-induced elevated input of nutrients.

Style Definition: Bullets: Indent: Left: 0 cm, First line: 0 cm, Bulleted + Level: 1 + Aligned at: 0.63 cm + Indent at: 1.27 cm, Tab stops: 0.63 cm, List tab

Style Definition: Normal (Web): Estonian, Left, Space Before: Auto, After: Auto, Line spacing: single

Formatted: English (United States)

Formatted: MS title, Space Before: 0 pt, Line spacing: single, Border: Top: (No border), Bottom: (No border), Left: (No border), Right: (No border), Between : (No border)

Formatted: Font: Not Bold, Font color: Auto, English (United States)

Formatted: English (United States)

Formatted: English (United States)

Formatted: English (United States)

1. ~~1~~ Introduction

Coastal dead zones have expanded in the oceans since the 1960s, a phenomenon which is mostly caused by increased primary production as a result of eutrophication (Diaz and Rosenberg, 2008). Geographic settings such as openness of the basin and hydrographic conditions such as the strength and onset of stratification affect the magnitude of near-bottom hypoxia (Codiga et al., 2009; Liblik et al., 2020b; Murphy et al., 2011; Ukrainskii and Popov, 2009; Zhang et al., 2010). Current and projected climate changes continue to affect the marine environment, e.g., increased temperature and strengthening of stratification in estuaries could lead to enhanced oxygen depletion of bottom waters (Bindoff et al., 2019).

The Baltic Sea is strongly influenced by eutrophication and changing climate conditions (Conley et al., 2009; Gustafsson et al., 2012; Kabel et al., 2012). ~~Drivers~~The primary drivers behind eutrophication are excessive amounts of nutrients~~, which~~ that enter the marine environment through rivers and the atmosphere~~. Rivers carry nutrients mainly originating from agricultural sources (e.g., fertilizers used in farming, leaching due to deforestations, etc.). Nutrients in the atmosphere are mostly from land-based sources (e.g., production of energy using fossil fuels, transport) but also from shipping (emission of nitrous oxide).~~

(HELCOM, 2018b). Hypoxic conditions have been found throughout the Baltic Sea as quasi-permanent, seasonal, or exceptional infrequent phenomena (Conley et al., 2007, 2011; Karlson et al., 2002). Hypoxia and anoxia ~~occur~~have occurred in ~~the~~ open water areas of the Baltic Proper below the halocline (~70-80 m) on an almost ~~permanently~~permanent basis since the 1950s (HELCOM, 2016; Karlson et al., 2002). ~~Oxygen~~Occasionally, oxygen conditions in ~~the near-bottom layer of deeper areas of the~~this central ~~Baltic Sea, where permanent halocline exists,~~basin are ~~occasionally~~ improved by Major Baltic Inflows (e.g., Matthäus and Franck, 1992; Schinke and Matthäus, 1998; Schmale et al., 2016; Liblik et al., 2018). ~~In the Gulf of Finland~~However, these improved oxygen conditions are short-lived because, in the long-term, the ~~south-westerly wind forcing could cause the reversal of estuarine circulation, leading to the collapse of~~inflows enhance stratification ~~in the cold season~~ and ~~subsequent oxygenation of sub-halocline layers~~thereby reduce vertical oxygen transport (~~Liblik~~Conley et al., ~~2013; Lips et al., 2017~~2002).

~~There are also~~ In the shallower regions, where the halocline is absent, but a seasonal thermocline restricts vertical mixing ~~and~~, oxygen consumption ~~leads~~could lead to temporal ~~hypoxia in the~~ near-bottom ~~layer~~ hypoxia and sediment phosphorus release in late summer-autumn~~, increasing the release of sediment phosphorus~~ (Lukkari et al., 2009; Puttonen et al., 2014, 2016; Walve et al., 2018). For instance, such seasonal hypoxic events ~~occur~~have occurred in the northern Baltic coastal areas and Åland archipelago, influenced by large-scale eutrophication driven by nutrients from agriculture and local fish farms (Bonsdorff et al., 1996). ~~Human-induced elevated~~Sedimentation of organic matter, stimulated by nutrient inputs ~~of nutrients~~, can cause severe oxygen deficiency ~~events in the case of certain~~under specific meteorological/hydrographic conditions, as ~~it happened~~

Formatted: Outline numbered + Level: 1 + Numbering Style: 1, 2, 3, … + Start at: 1 + Alignment: Left + Aligned at: 0 cm + Indent at: 0.63 cm

Formatted: English (United States)

Field Code Changed

Formatted: English (United States)

Formatted: English (United States)

Formatted: English (United States)

Formatted: English (United States)

Formatted: English (United States)

Formatted: English (United States)

Formatted: English (United States)

~~in 1994 and 2002~~observed in the southern Baltic in 1994 and ~~the Danish coastal waters~~2002 (e.g. Conley et al., 2007; Powilleit and Kube, 1999).

One of the shallow areas~~,~~ where seasonal hypoxia ~~occasionally occurs,~~can occur is the Gulf of Riga (GoR) in the eastern part of the Baltic Sea (e.g., Berzinsh, 1995 and references therein; Aigars and Carman, 2001; Eglīte et al., 2014; Aigars et al., 2015). The Gulf of Riga is a semi-enclosed ~~shallow~~ basin (Fig. 1) with a surface area of 16,330 km^2, a volume of 424 km^3, and a mean depth of 26 m (Ojaveer, 1995; HELCOM, 2002). ~~The gulf's~~Its deeper central area, situated east of the Ruhnu island, has depths of up to 56 m (Stiebrins and Väling, 1996). ~~Water~~The water and salt ~~budget~~budgets of the gulf ~~if~~are governed by river discharge, precipitation-evaporation balance, and water exchange with the Baltic Proper through the connecting straits. The long-term (1950–2015) mean river runoff is about 36 km^3 year^{-1} (Johansson, 2016), and the average freshwater flux due to the difference between the surface precipitation and evaporation rates is about 2.5 km^3 year^{-1} (Omstedt et al., 1997). Five larger rivers (Daugava, Lielupe, Gauja, Pärnu, and Salaca) enter the southern and eastern part of the gulf ~~whereas~~, with the Daugava river ~~contributes~~contributing about 70% ~~to~~of the total riverine input (Yurkovskis et al., 1993). Assuming the gulf's water volume and salt ~~content's~~content annual balance, Lilover et al. (1998) estimated ~~the~~that its water renewal period would be about three years.

GoR water exchange with the Baltic Proper takes place via the Irbe Strait in the west (about 70-80% of water exchange) and the Suur Strait in the north ~~(Petrov, 1979).~~(Astok et al., 1999; Petrov, 1979). The Irbe Strait has a sill depth of 25 m and a cross-section area of 0.4 km^2, while ~~the Suur Strait~~these hydrographical features are 5 m and 0.04 km^2, respectively, for the Suur Strait. Lips et al. (1995) suggested that the ~~gulf~~gulf's deep layer water could be renewed in summer by inflows of saltier water from the eastern Baltic Proper over the sill in the Irbe Strait~~,~~ – which is deeper and wider~~,~~ – while inflows through the shallow Suur Strait are arrested in the surface layer. The near-bottom inflows through the Irbe Strait are intensified by the northerly and north-easterly winds ~~that~~, which cause upwelling events along the eastern coast of the Baltic Proper. Model simulations by Raudsepp and Elken (1995) also showed that strong northerly wind events could create substantial near-bottom inflows of saltier Baltic Proper waters. However, when downwelling occurs along the eastern coast of the Baltic Proper, the inflowing water is warmer than that of the near-bottom layer water in the Gulf of Riga in summer, and ~~it~~ can spread buoyantly at the intermediate depths (Liblik et al., 2017). ~~A general cyclonic circulation in the Gulf of Riga with the southward flow on the western side and northward flow on the eastern side of the gulf was described by Yurkovskis et al. (1993). In accordance with this flow scheme, freshwater from the south-eastern part of the gulf moves toward the north along the eastern shore in the surface layer while the inflowing saltier water through the Irbe Strait moves toward the south as a geostrophically balanced gravity current along the gulf's western slope. The numerical study by Lips et al. (2016) suggested a more complicated (seasonally altered) whole-basin circulation in the surface layer depending on the prevailing wind forcing and stratification.~~

Formatted: English (United States)
Formatted: English (United States)
Formatted: English (United States)
Formatted: English (United States)
Formatted: English (United States)

Because of the shallowness of the basin, the ~~whole~~entire water column is well mixed ~~and vertical distributions of temperature, salinity and oxygen are homogenous~~ in winter. In summer, stratification is mainly maintained by the seasonal thermocline, which ~~starts to develop~~begins developing in April and is ~~the~~at its strongest in August, ~~and~~while the contribution of haline stratification is ~~rather~~relatively moderate (Stipa et al., 1999; Liblik et al., 2017). Based on CTD profiles from 1993–2012, Skudra and Lips (2017) revealed ~~based on summer CTD profiles from 1993–2012~~ that the strongest stratification ~~of water column~~ occurred in the years with the highest ~~upper layer~~summer surface temperature ~~in summer~~ and spring river ~~runoff in spring. High~~discharge. A high correlation between the deep layer salinity in the Irbe Strait and the gulf was found by ~~Skudra and Lips, (2017)~~Skudra and Lips (2017), in accordance with the suggestion that the majority of water exchange between the Baltic Proper and the gulf occurs through the Irbe Strait.

~~The general annual cycle of dissolved oxygen (DO) concentration in the Gulf of Riga could be described as follows (Berzinsh, 1995 and references therein): in the surface layer, oxygen concentrations are close to the saturation in winter, maximum concentrations are observed during the vernal phytoplankton bloom in late April and early May, and a decrease in the surface layer oxygen concentrations appears due to the decay of the spring bloom and increasing water temperature in summer; oxygen conditions in the near-bottom layer are influenced by the amount of decomposing organic material, lateral transport, and mixing in the water column, the lowest concentrations are observed in late summer and autumn and the maximum close to saturation in winter when the water column is completely mixed.~~

Based on data from 1963 to 1990, a statistically significant decreasing trend of oxygen concentration in August was found for the entire 20–50 m layer in the gulf (Berzinsh, 1995). No trend was detected after that (HELCOM, 2009). The latest monitoring data are not analyzed for long-term trends and inter-annual variations in near-bottom oxygen concentrations; ~~instead~~rather, model outcomes are used to describe the oxygen conditions (e.g., Jansson et al., 2020). ~~However, it~~It is well documented, however, that the anoxic and hypoxic areas have been expanding in the entire Baltic Sea ~~during the last~~in recent decades, due to both eutrophication and ~~the~~ changes in climatic conditions (Hansson and Viktorsson, 2020; the analysis also ~~includes data from the Gulf of Riga). For a northern Baltic coastal basin, it has been suggested that in addition to the anthropogenic nutrient input the shoaling of the basin and warming contributed to the deoxygenation of bottom waters (Jokinen et al., 2018). Otherwise, it was impossible to explain more frequent seasonal hypoxia occurrences since the beginning of the 1900s.~~included data from the Gulf of Riga).

Total annual nitrogen and phosphorus loads to the Gulf of Riga estimated for 2017 at levels of 90 544 and 2 427 t year^{-1}, respectively, and are still higher than the maximum allowable inputs, according to the Baltic Sea Action Plan~~, and almost no trends in inputs have been observed compared to the reference period 1997–2003~~ (HELCOM, 2019). Based on monitoring data since 1974, the phosphorus pool in the Gulf of Riga constantly increased ~~till~~until the mid-1990s (Yurkovskis, 2004)~~; afterward, a tendency has been unclear (HELCOM, 2018b). Since the phosphorus delivery by rivers is <15% compared to its~~

Formatted: English (United States)

Formatted: English (United States)

Formatted: English (United States)

~~pool (Yurkovskis, 2004).~~, and was followed by stagnation (HELCOM, 2018a). Since riverine phosphorus input is <15% compared to phosphorus pool in the water column (Yurkovskis, 2004), the changes in the latter are largely governed by internal processes. The phosphate flux from the sediments to the water column depends on the near-bottom oxygen conditions with maximum values at low DO concentrations. For instance, ~~values~~phosphorus release in the order of 100 µmol PO_4^{3-} m^{-2} d^{-1} ~~were~~was simulated at oxygen concentrations 1-2 mg l^{-1} (Eglīte et al., 2014). Thus, the reoccurrence of ~~poor~~low near-bottom oxygen conditions supports sediment phosphorus release ~~that~~which counteracts potential decreases in the external phosphorus load to the gulf.

~~The Gulf of Riga experienced extensive near-bottom hypoxia in summer-autumn 2018. This study aims to evaluate the possible role of different forcing factors leading to the observed hypoxia. For that, we analyzed the dissolved oxygen, stratification and forcing data in 2018 and compared these with the long-term means and variability. A more detailed comparison with the conditions in 2017, when hypoxia did not develop, was conducted. In addition, we estimated the oxygen consumption rates and sediment phosphorus release under the observed hypoxic conditions.~~

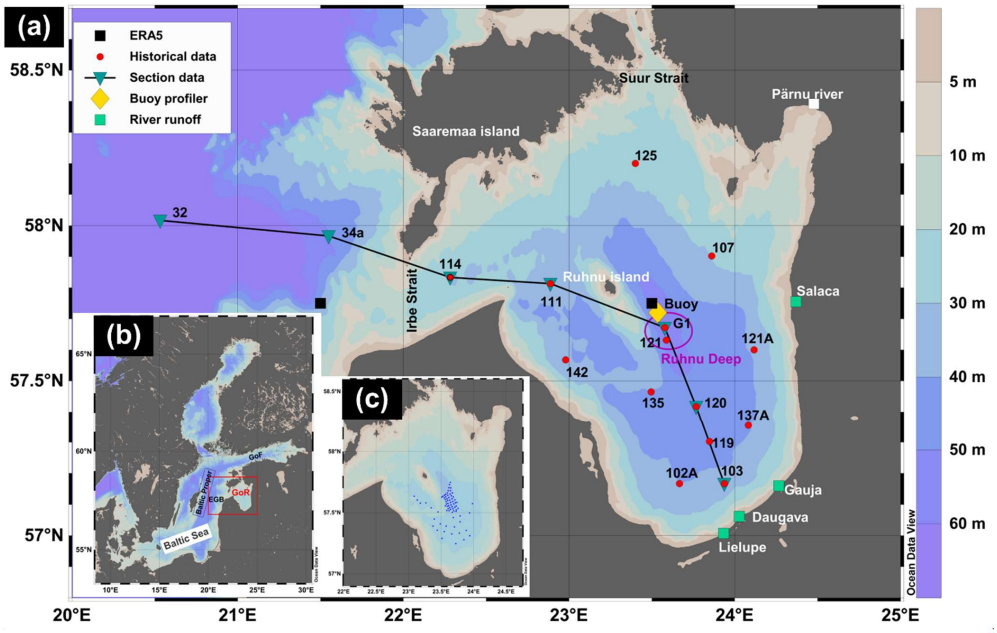

Formatted: English (United States)

Data from regular monitoring cruises and targeted surveys revealed extensive near-bottom hypoxia in the Gulf of Riga in summer-autumn 2018. Additionally, the weather conditions were extreme in summer 2018, manifested by a new air temperature maxima in Europe for April-September (Hoy et al., 2020). We have formulated three main questions for this study: Was the observed near-bottom hypoxia in the GoR in 2018 an exceptional event? What were the reasons behind the observed hypoxia? Was it a feature that could occur in the GoR and similar basins regularly and/or even more often in the future? We hypothesize that the earlier onset, strength, and duration of stratification, together with the unusually high winter river runoff, were the main contributors to the extensive near-bottom hypoxia in 2018. If this hypothesis holds, then one may predict that the future occurrences of such events will likely increase. To test our hypotheses, we analyzed oceanographic and meteorological conditions in 2018, and compared them with the preceding years (2012-2017) and long-term means and variability.

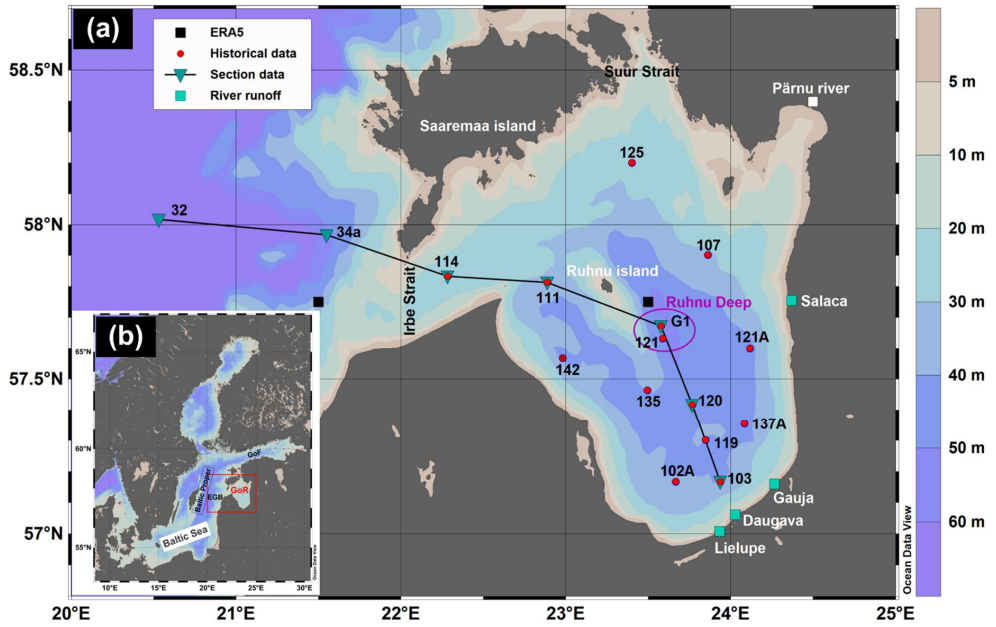

Figure 1. (a) - Map of the study area in the Gulf of Riga (GoR) with bottom topography. Red-filled circles represent the locations of monitoring stations. ~~Yellow filled diamond represents the location of buoy profiler.~~ Inverted triangles represent the stations used for section figures. Black-filled squares represent the grid cell center points of ERA5 data (grid cell resolution 0.25º x 0.25º). Green-filled squares ~~mark~~denote rivers from where runoff data ~~were~~was used. EGB – Eastern Gotland Basin,

and GoF – Gulf of Finland. (b) – Study area in the Baltic Sea. ~~(c) – Survey stations in September, 2018.~~ This map was generated using Ocean Data View 5.2.0 software (Schlitzer, 2019).

2. ~~2~~ Material and methods

~~Data sets~~Historical data on the near-bottom temperature, salinity, dissolved oxygen, and nutrient concentrations were downloaded from ~~various sources covering different periods with different~~the Estonian environmental monitoring information system (KESE), Latvian environmental monitoring databases, ICES/HELCOM database, and SeaDataNet Pan-European infrastructure for ocean and marine data management (http://www.seadatanet.org). More consistent near-bottom oxygen data were available from 2005; therefore, we limited the analysis to 2005–2018. HELCOM guidelines (HELCOM, 2017) were followed for the sampling~~/recording frequencies were used.~~ and analytical detection of oxygen and nutrient concentrations in the monitoring laboratories.

Vertical profiles of temperature, salinity, and dissolved oxygen with temporal resolution of at least six times a year are available since 2012. The profiles were recorded using an Ocean Seven 320plus CTD probe (Idronaut s.r.l.) onboard r/v Salme during Estonian and Latvian monitoring cruises ~~in 2012–2018~~ (stations are shown in Fig. 1). Salinity and density anomaly are shown in the present study as Absolute Salinity (g kg^{-1}) and Sigma-0 (kg m^{-3})), and were calculated using the TEOS-10 formula (IOC et al., 2010). The oxygen sensor (Idronaut s.r.l.) attached to the OS320plus probe was calibrated ~~before~~prior to each cruise. Oxygen profiles used for the analysis were quality ~~-~~checked against the laboratory analysis of water samples using an OX 400 l DO (WWR International, LCC) analyzer. The accuracy of the Idronaut oxygen sensor is 0.1 mg l^{-1}, while the accuracy of the laboratory dissolved oxygen analyzer is 0.5 % of the measured value. The primary data set~~, from where~~ used to characterize the ~~vertical profiles~~water column structure and ~~sections were drawn and~~ dissolved oxygen ~~consumption estimated~~,and phosphates concentrations in 2018 was collected ~~within the following six campaigns in 2018:~~on 9-10 January, 17-18 April, 30 May, 11 July, 25 August, and 26-27 October.

~~Nutrient concentrations were determined from water samples collected onboard r/v Salme during monitoring cruises in 2018 using the automatic nutrient analyzer Lachat QuikChem 8500 Series 2 (Lachat Instruments, Hach Company). The nutrient analyses were performed according to the recommendations by USEPA, ISO, and DIN standards (methods 31-107-04-1-D NO_3 (Egan, 2000) and 31-115-01-1-I PO_4 (Ammerman, 2001)). The lower detection range for PO_4^{3-} and $NO_2^- + NO_3^-$ was 0.06 and 0.08 µM, respectively.~~

~~High-frequency measurements were carried out with a buoy profiler in the gulf's deepest part in summer 2018 (Fig. 1). The profiler system Mona (Flydog Solutions Ltd.) recorded vertical profiles of temperature, salinity, dissolved oxygen, and chlorophyll-a fluorescence eight times a day from 5 to 21 August. It includes an OS316plus CTD probe (Idronaut s.r.l.) with an Idronaut oxygen sensor and Trilux fluorescence sensor (Chelsea Technologies Group Ltd.). The profiler records data at a rate of 8–9 Hz while moving down with an average speed of 8–10 cm s^{-1}. The accuracy of the used Idronaut oxygen sensor is~~

Formatted: Outline numbered + Level: 1 + Numbering Style: 1, 2, 3, … + Start at: 1 + Alignment: Left + Aligned at: 0 cm + Indent at: 0.63 cm

~~0.1 mg l^{-1}. After the pre-processing of data, the vertical profiles were stored with a constant step of 0.5 m from 3 m to 50 m. Data from the research vessel cruises were used for the quality assurance of the measurements by the buoy profiler.~~

~~Historical data on temperature, salinity, dissolved oxygen, and nutrient concentrations were obtained from the Estonian environmental monitoring information system (KESE), Latvian environmental monitoring databases, ICES/HELCOM database, and SeaDataNet Pan-European infrastructure for ocean and marine data management (http://www.seadatanet.org) for the period 2005–2018.~~

~~Meteorological data for two locations were extracted from the ERA5 dataset via Copernicus Services (see in Fig.1; a grid cell has horizontal dimensions of 0.25ºx0.25º) (Hersbach et al., 2018). Hourly net solar radiation and wind data at the 10 m height from the grid cell centered at 57º30′ N, 23º30′ E in the gulf from 1979 to 2018 were obtained to characterize local conditions. Surface net solar radiation (J m^{-2}) is the amount of solar radiation (shortwave radiation) reaching the surface of the Earth (both direct and diffuse) minus the amount reflected by the Earth's surface. Also, hourly wind data at the 10 m height from the grid cell centered at 57º 30′ N, 21º 30′ E (outside the gulf) for March–August 2017 and 2018 were extracted to find the periods with upwelling-favorable conditions along the eastern coast of the Baltic Proper.~~

~~River runoff data (1993–2018) were received from the Latvian Environment, Geology and Meteorology Center and contain the estimated monthly runoff ($m^3 \cdot s^{-1}$) of rivers Salaca, Gauja, Lielupe, and Daugava (Fig 1). River runoff is presented as monthly average flow ($m^3 \cdot s^{-1}$) per river.~~

~~Oxygen concentration ≤ 2.9 mg l^{-1} was used as the threshold concentration for hypoxia, and the upper boundary of the hypoxic layer was found as the minimum depth where oxygen concentration was below the threshold. The estimated depth of the upper boundary of the hypoxic layer at station G1 (see Fig. 1) and the gridded topography (EMODnet Bathymetry Consortium, 2020) were used to find the lateral extent of the hypoxic area. In 2018, special surveys were conducted in the gulf's central deeper area, and the area of hypoxic near-bottom water was also estimated using the survey mean depth of the hypoxic layer upper boundary.~~

The depth of the upper mixed layer (UML) was defined according to Liblik and Lips (2012) as the minimum depth, where $\rho_z - \rho_3 > 0.25$ kg m^{-3}, where ρ_z is the density anomaly at depth z and ρ_3 at depth 3 meters. The depth of the near-bottom mixed layer (NBL) was found similarly to UML, as the maximum depth, where $|\rho_z - \rho_{last}| > 0.1$ kg m^{-3}, where ρ_{last} is the density anomaly at the maximum depth of a profile. Oxygen concentration ≤ 2.9 mg l^{-1} (2 ml l^{-1}) was used as the threshold concentration for defining hypoxia, and the upper boundary of the hypoxic layer was found as the minimum depth at which oxygen concentration was below the threshold. The estimated depth of the upper boundary of the hypoxic layer at station G1 and the gridded topography (EMODnet Bathymetry Consortium, 2020) were used to find the lateral extent of the hypoxic area,

assuming that the border of hypoxia was spatially horizontal. The sea depth at station G1 is 54 m (Fig. 1). The profiles covered – in most cases – the depth range from 2 to 52 m. The water column structure was characterized by temperature, salinity, and density in the UML and NBL and potential energy anomaly (PEA; Simpson et al., 1990) calculated as

~~We introduce a rough method estimating oxygen consumption rates in the gulf NBL. If neglecting mixing between the NBL and the water column above it, salinity changes in the NBL should be attributed to the lateral advection and mixing of the NBL water with the inflowing waters. Knowing salinities of inflowing waters and gulf NBL waters at time steps *t1* ("old" water) and *t2* ("new" water), we can estimate the proportion of inflowing waters in the near-bottom water mass at time step *t2*. Using this proportion, we can also estimate the expected changes in the NBL oxygen concentration due to lateral transport and mixing. The expected oxygen concentration of the "new" water can be found as~~

~~$$O_z^{t2}(G1) = O_z^{t1}(G1) + \left(O_z^{t1}(114) - O_z^{t1}(G1)\right) * \left[\frac{Sal^{t2}(G1) - Sal^{t1}(G1)}{Sal^{t1}(114) - Sal^{t1}(G1)}\right], \quad (1)$$~~

~~where the parameters of the "old" water are defined as salinity and oxygen concentration at an initial time step *t1* in the NBL at station G1 ($Sal^{t1}(G1)$ and $O_z^{t1}(G1)$, respectively) and the inflowing water as salinity and oxygen concentration in the NBL at station 114 in the Irbe Strait ($Sal^{t1}(114)$ and $O_z^{t1}(114)$, respectively; see Fig. 1). $Sal^{t2}(G1)$ is salinity of the "new" water defined as salinity in the NBL at station G1 at time step *t2*.~~

~~To account for the changes in the NBL salinity and oxygen concentration due to vertical mixing between the NBL and upper water layers, we used a similar approach as by Stoicescu et al. (2019). Diffusive flux through the border between the NBL and the water column above can be estimated based on the vertical gradient of salinity~~

$$PEA = \frac{1}{h}\int_{-h}^{0}(\bar{\rho} - \rho)gzdz, \quad \text{where } \bar{\rho} = \frac{1}{h}\int_{-h}^{0}\rho dz, \quad (1)$$

where h is the water column depth (50 m), ρ is water density, z is depth (vertical coordinate), and $g = 9.81\ m\ s^{-2}$.

Meteorological data for 1979-2018 were extracted from the ERA5 dataset (Hersbach et al., 2018) via Copernicus Services for characterizing local conditions in the gulf and upwelling-favorable conditions along the eastern coast of the Baltic Proper. Based on hourly data from a grid cell in the central gulf (see Fig.1), the monthly mean net solar radiation, air temperature (2 m above surface) and wind speed (at the 10 m height) in 2018 were calculated and compared with monthly mean values and variability in 1979–2018. River runoff data were received from the Latvian Environment, Geology and Meteorology Center and contained the estimated monthly runoff ($m^3\ s^{-1}$) of rivers Salaca, Gauja, Lielupe, and Daugava (Fig. 1) in 1993–2018.

For a more detailed analysis of the impact of meteorological and hydrological conditions on the development of stratification, changes in potential energy anomaly due to surface heating-cooling (S_b), wind mixing (S_m), and freshwater discharge from rivers (S_r) were estimated for the years 2012-2018

$$\frac{dPEA}{dt} = S_b + S_m + S_r. \quad (2)$$

The two former parameters were calculated as suggested by (Simpson et al., 1990)

$$S_b = \frac{\alpha_v g Q_{TOT}}{2c_p} \text{ and } S_m = -\delta C_D \rho_a \frac{W^3}{h}, \quad (3)$$

where Q_{TOT} is the surface heat flux and W is the wind speed. Q_{TOT} is the sum of the shortwave radiative heat flux, longwave radiative heat flux, sensible heat flux, and latent heat flux estimated using ERA5 data and surface salinity obtained from CTD casts interpolated between the measurements. Thermal expansion coefficient α_v was calculated using the TEOS-10 formula (IOC et al., 2010) and specific heat of seawater $c_p = 4000\ J\ (kg\ K)^{-1}$ was applied. In the formula for the shortwave radiative heat flux, an average albedo of 0.055 was used (Groeskamp and Iudicone, 2018; Séférian et al., 2017). Otherwise, we used the same methods of calculating surface heat flux components as Liblik and Lips (2012). For estimating S_m, constant values of efficiency of mixing $\delta = 10^{-3}$ and air density $\rho_a = 1.25\ kg\ m^{-3}$ were applied and effective drag coefficient C_D was calculated according to (Wu, 1982). The changes in stratification due to river discharge were estimated using monthly runoff from the previous month. The flow in $m^3\ s^{-1}$ was multiplied by a constant, which was found assuming that the average yearly change in PEA in 2012-2018 was equal to the change caused by the average runoff of 36 km $year^{-3}$ evenly distributed over the entire surface area of the gulf.

Wind data from a grid cell outside the gulf, but close to the Irbe Strait (see Fig. 1), were extracted to calculate the north-northeast (NNE) component of wind stress as $\tau_{NNE} = C_D \rho_a |W| W_{NNE}$, where W_{NNE} is the wind speed component directed towards NNE (south-southwest wind component). It is used to find the periods with upwelling-favorable conditions along the eastern coast of the Baltic Proper and for a more detailed analysis of inflows-outflows through the Irbe Strait in 2012-2018.

We introduce a rough method estimating oxygen consumption rates in the gulf NBL. The considered physical processes contributing to the measured changes in salinity and oxygen concentration in the NBL were: 1) vertical diffusion and 2) lateral advection and mixing. Diffusive flux of salt and oxygen through the border between the NBL and the water column above was estimated using a similar approach as Stoicescu et al. (2019)

$$DIFF_S = -k * \frac{\partial S}{\partial z} \frac{\partial S}{\partial z} \text{ or oxygen and } DIFF_{O_2} = -k * \frac{\partial O_2}{\partial z}, \frac{\partial O_2}{\partial z}, \quad (4)$$

where the vertical diffusivity coefficient is calculated as $k = \frac{\alpha}{N} \frac{\alpha}{N}$, α is the empirical intensity factor of turbulence (we applied a constant value $\alpha = 1.5 * 10^{-7}\ m^2\ s^{-2}$)), and N is the Brunt-Väisälä frequency defined by the vertical density gradient. The changes in salinity and oxygen concentration in the NBL can be found by multiplying the valuesvalue of diffusive fluxes with the time between two measurements ($t2$-$t1$) and dividing it with the thickness of the NBL (h_{NBL}). As a consequence, salinity at station G1 at time step t2 used in Eq. 1 should be found by subtracting from the measured salinity value ($Sal^{t2m}(G1)$) the estimated change due to diffusion) as $Sal^{t2}(G1) = Sal^{t2m}(G1) - DIFF_s * (t2 - t1)/h_{BNL}$.

$$\Delta S^{DIFF} = DIFF_S * \frac{t2-t1}{h_{NBL}} \text{ and } \Delta O_2^{DIFF} = DIFF_{O_2} * \frac{t2-t1}{h_{NBL}}. \quad (5)$$

Knowing salinities of inflowing waters and gulf NBL waters at time steps *t1* and *t2* and the changes due to vertical diffusion, we can estimate the proportion of inflowing waters in the near-bottom water mass at time step *t2*. Using this proportion, we can also estimate the expected changes in the NBL oxygen concentration due to lateral transport and mixing as

$$\Delta O_2^{ADV} = \left(O_2^{t1}(114) - O_2^{t1}(G1)\right) * \left[\frac{Sal^{t2}(G1) - Sal^{t1}(G1)}{Sal^{t1}(114) - Sal^{t1}(G1)}\right], \quad (6)$$

where $Sal^{t1}(G1)$ and $O_2^{t1}(G1)$ are salinity and oxygen concentration in the NBL at station G1 and $Sal^{t1}(114)$ and $O_2^{t1}(114)$ at station 114 in the Irbe Strait (see Fig. 1) at an initial time step *t1*. $Sal^{t2}(G1)$ is measured salinity in the NBL at station G1 at time step *t2* corrected by the estimated salinity change due to vertical diffusion.

Due to oxygen consumption, measured oxygen concentration in the NBL at station G1 at time step *t2* ($O_2^{t2m}(G1)$) should be lower than that found when considering only changes due to physical processes ~~(lateral advection and mixing, estimated by Eq. 1 and vertical diffusion)~~ since no production is expected in the near-bottom layer that is well below the euphotic depth. ~~Dividing the difference between the expected and measured oxygen concentration by the time between two measurements (*t2-t1*), we can estimate the oxygen~~Oxygen depletion ~~rate~~ due to consumption~~. Oxygen consumption per unit bottom area is calculated~~ can be found as the sum of the measured oxygen depletion and changes in concentration due to diffusion and lateral advection and mixing

~~$O_2^{consumptio} = \left(O_2^{t2}(G1) - O_2^{t2m}(G1)\right) / (t_2 - t_1) * h_{NBL} + DIFF_{O_2}$.~~ (2)

$$\Delta O_2^{CONS}(G1) = -(O_2^{t2m}(G1) - O_2^{t1}(G1)) + \Delta O_2^{DIFF} + \Delta O_2^{ADV}. \quad (7)$$

Oxygen consumption rate per unit bottom area is calculated as

$$O_2^{CONS\ rate} = \frac{\Delta O_2^{CONS}}{t_2 - t_1} * h_{NBL}. \quad (8)$$

We have chosen the time step of one month or longer to estimate oxygen consumption rates based on the distance between the Irbe Strait and the Ruhnu Deep (120 km, measured along the deeper area of the gulf) and average (monthly) flow rates in the gulf of 5 cm s^{-1} (e.g., Soosaar et al., 2014; Lips et al., 2016). The applicability of the introduced consumption rate estimates is more thoroughly analyzed in the Discussion ~~section.~~(Sect. 4).

The same ~~approach of using the changes in salinity for defining the proportion of water masses in the mixture was~~methods were used to estimate ~~the flux of phosphates~~phosphate fluxes due to physical processes and phosphorus release from the sediments. The measured concentrations in the near-bottom layer at station G1 were assigned to the gulf's water and at station 114 to the inflowing water. In Eqs. (~~1) and (2~~4) – (8), oxygen concentration was replaced by phosphate concentration~~. The~~ and the difference in measured and expected phosphate concentrations in the gulf near-bottom layer was associated with the phosphorus release from the sediments.

~~1. 3~~ Since the vertical resolution of nutrient~~Results~~

~~3.1. Inter-annual and seasonal variability~~

~~3.1.1. Inter-annual and seasonal changes in near-bottom oxygen and phosphate concentrations~~

~~Data at the central, deep stations G1 and 121 (see Fig. 1; further on, these stations are treated as one station) in 2005–2018 showed high variability of oxygen concentration in the near-bottom layer (Fig. 2). High oxygen concentrations were measured in winter when the gulf's water column was well mixed. Seasonal hypoxia in the near-bottom layer was occasionally registered in several years from August to November. No hypoxia was observed in 2006–2011 (except one value close to 2.9 mg l^{-1} in 2009), but note the scarce sampling frequency. Using the series of the deepest, simultaneously measured salinity and oxygen content values at station G1 from August to November in 2005-2018, we found a statistically significant ($p < 0.05$, $R^2 = 0.21$, $n = 35$) negative relationship – low oxygen values correspond to high salinity values. However, there were examples when hypoxia occurred at salinities slightly above 5.5 g kg^{-1} (in 2015) and did not exist at salinities 6.5 g kg^{-1} (in 2010).~~

~~We estimated temporal trends in the average summer (August) and autumn (October-November) near-bottom oxygen and phosphate concentrations using data from 2005-2018 at all stations with depth >= 40 m (see station locations in Fig. 1). A statistically significant ($p < 0.05$) decreasing trend in dissolved oxygen at a rate of 0.45 mg l^{-1} $year^{-1}$ was found in autumn ($n = 13$, $R^2 = 0.50$). Statistically significant increasing trends were found for the near-bottom phosphate concentration in summer (0.08 µM $year^{-1}$, $n = 14$, $R^2 = 0.47$) and autumn (0.12 µM $year^{-1}$, $n = 13$, $R^2 = 0.34$). As expected from these results, statistically significant negative correlation was obtained between the autumn near-bottom layer mean oxygen and phosphate concentrations ($n = 13$, $R^2 = 0.79$). The autumn near-bottom layer oxygen also significantly correlated with the next year winter (January) near-bottom layer phosphate concentration ($n = 9$, $R^2 = 0.59$).~~

Formatted: Outline numbered + Level: 1 + Numbering Style: 1, 2, 3, … + Start at: 1 + Alignment: Left + Aligned at: 0 cm + Indent at: 0.63 cm

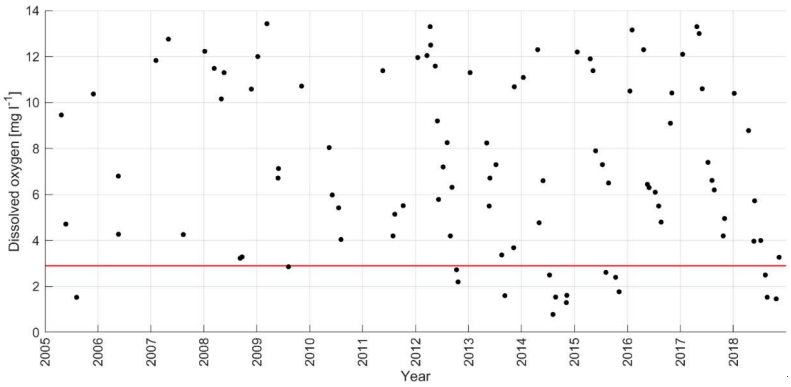

Figure 2. Inter-annual variability of near-bottom dissolved oxygen concentration using the deepest measured values at monitoring stations G1 and 121 in 2005–2018. A bold red line marks the oxygen concentration 2.9 mg l^{-1} (threshold concentration for hypoxia).

3.1.2. Inter-annual and seasonal variability in vertical distribution of temperature, salinity, density, and oxygen

Time series of the vertical distributions of temperature, salinity, density anomaly, and oxygen concentration at monitoring station G1 in 2012–2019 are presented in Fig. 3. A clear seasonal course was observed in all parameters. During the cold season, when the water column was practically mixed, the lowest temperatures and largest oxygen concentrations were observed (Fig. 3a and d). Inter-annual changes in the summer (June-September) UML temperature and depth as well as vertical stratification were large, most probably due to the variation in atmospheric forcing (surface heat flux and wind stress). UML was deeper in the summers 2012 and 2017, and mean surface layer temperatures were higher (23.5 °C) in 2014 and (22.4 °C) in 2018 (Fig. 3a). Lower mean surface layer salinities (5.2-5.3 g kg^{-1}) were observed in 2012, 2013, 2014 and 2018 (Fig. 3b). Increased salinity in the near-bottom layer was observed in the summers 2013 (6.3-6.5 g kg^{-1}) and 2018 (6.5-6.8 g kg^{-1}) (Fig. 3b), indicating saline water inflows from the Baltic Proper into the gulf through the Irbe Strait. The low salinity in the surface layer and the saline water inflows contributed to the strongest water column stratification in these years (Fig. 3c) – the density difference between the bottom and surface layer was 2.6 kg m^{-3} and 2.8 kg m^{-3} in 2013 and 2018, respectively. The weakest stratification was in 2012 and 2017 when the respective density difference was 1.5 kg m^{-3}.

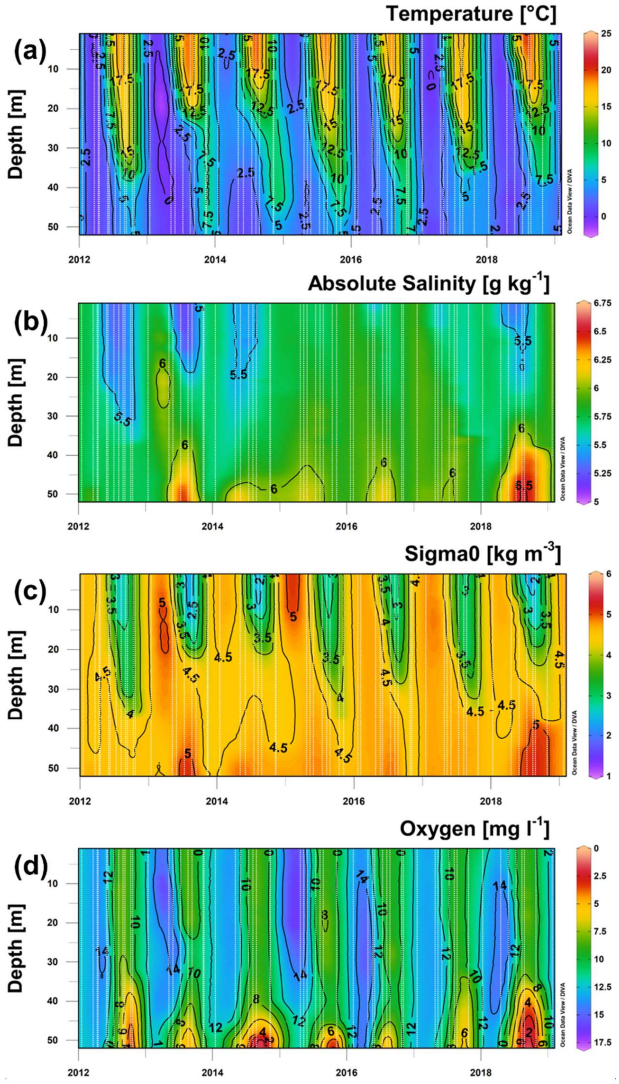

Figure 3. Time series of the vertical distribution of temperature (a), salinity (b), density anomaly (c), and oxygen concentration (d) at stations G1 and 121 in 2012-2019. Vertical white dashed lines mark the time of measured profiles.

The lowest oxygen concentrations, below the hypoxia threshold, were observed in the near-bottom layer in summer/autumn 2012 (2.2 mg l^{-1}), 2014 (0.8 mg l^{-1}), 2015 (1.8 mg l^{-1}) and 2018 (1.5 mg l^{-1}) (Fig. 3d). The bottom area covered by hypoxic waters, estimated using the profiles measured at station G1, was up to 4.4% (703 km^2) in 2012, 2.4% (382 km^2) in 2014, and 2.1% (338 km^2) in 2015. The estimated extent of hypoxia was the largest in 2018 when the hypoxic water covered 5.2% (834 km^2) of the gulf's bottom area.

The hypoxic area was also estimated using the survey data from September 2018 instead of a single profile (see panel C in Fig. 1). Profiles with a minimum depth of ≥ 45 m were selected (n = 50). The mean depth, where DO concentration was 2.9 mg l^{-1}, was 44.5 m, corresponding to a hypoxic area of 935 km^2 (5.9%). Hypoxia was detected in 92% of the selected profiles. Hypoxic depth values varied from the mean with a standard error of 2.1 m, and the coefficient of variation was < 4 %. These estimates show that the survey data gave the estimate of the hypoxic area close to the estimate using only the oxygen profile at a central station. Vertical profiles at station G1 acquired in August and October both gave the estimate of 834 km^2 while the survey in September 935 km^2. The latter points to a maximum hypoxia extent in September, between the regular environmental monitoring cruises in August and October. Using the dense survey data, we can get confidence limits for hypoxic depth estimates from a single profile considering the detected ca 4 % variation of the results.

3.2 Analysis of long-term forcing data

3.2.1 Wind conditions

We compared wind conditions in 2018 with the long-term mean wind conditions by calculating monthly mean wind vectors for 1979–2018 and 2018 from ERA5 wind data (Fig. 4a). For this analysis, the data point located in the EGB (see Fig. 1) was used. Mean wind vectors in February, March, May, July and September in 2018 differ considerably from the long-term mean wind vectors. North-easterly winds supporting the inflow of saline water from the Baltic Proper through the Irbe Strait into the gulf prevailed in February-March, May and July 2018. In September 2018, south-westerly winds prevailed, but the magnitude was larger than usual. To characterize wind-induced mixing, we also compared the monthly average wind speed in 2018 with the wind speed statistics for the period 1979-2018 (Fig. 4b). Here, the data point located in the Gulf of Riga (see Fig. 1) was used. The monthly average wind speed from February to August was lower in 2018 than the average for the respective month, except in April. The lowest wind speed for the entire period 1979-2018 was found in May 2018, suggesting that the wind-induced mixing of the water column in May was the weakest in 2018 if compared with the other years.

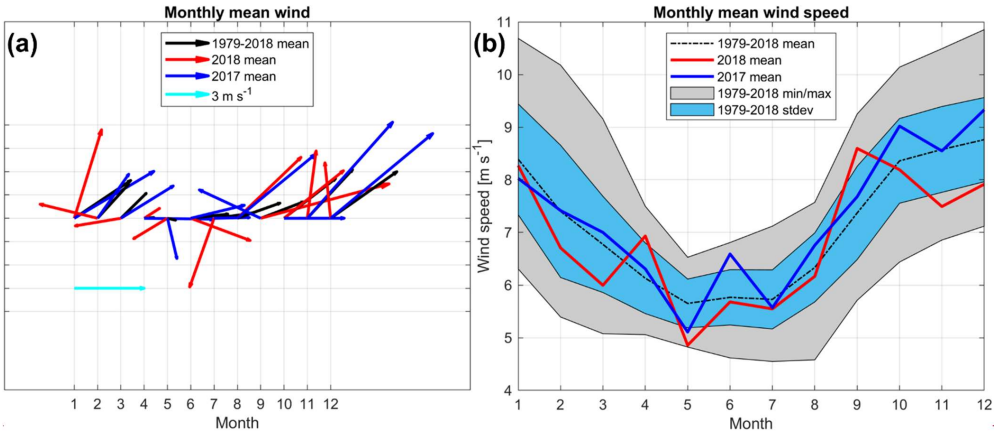

Figure 4. (a) Monthly mean wind vectors in 1979–2018 (black arrows), 2017 (blue arrows) and 2018 (red arrows) in the EGB close to the Irbe Strait. (b) Monthly mean wind speed with standard deviation and minimum-maximum values of monthly mean wind speed in 1979–2018 and monthly mean wind speed in 2017 and 2018 in the central Gulf of Riga (see locations of grid cells in Fig. 1).

Formatted: English (United States)

To find similar years to the year 2018 in terms of prevailing north-easterly winds, we analyzed monthly mean wind vectors in 2005–2017, when we have regular dissolved oxygen measurements in the Gulf of Riga. Although the winds were predominantly from the south-westerly direction in 1979–2018, northerly (from north-west to north-east) winds were observed for 1–2 months in spring–summer for several years in 2005–2018. These years and months were 2005 (March – NNE, April and June – WNW), 2006 (March – NE, July – NW), 2008 (April – NE, May – N), 2009 (April – WNW, June – NNW), 2010 (May – NNE), 2011 (April – NW), 2012 (March – NW), 2013 (March – NE, July–NW), 2014 (May and June – NW) and 2015 (April – WNW). The years with no dominating winds from northerly direction were 2007, 2016 and 2017. Low oxygen concentrations in the near-bottom layer of the central gulf were observed in the late summer–autumn of 2005, 2012–2015 and 2018 (Fig. 2). Thus, the anomalous winds in spring–early summer are a characteristic feature for the years when low oxygen concentrations occurred in late summer–autumn, but such winds alone were not sufficient for causing the hypoxia.

3.2.2 River runoff

Analysis of monthly mean river runoff data (sum of rivers Salaca, Gauja, Lielupe, and Daugava) showed considerable variability, especially in spring (March–May) (Fig. 5). A comparison of monthly river runoff values from the year 2018 with the long-term mean values (1993–2018) shows that runoff was mostly lower than the long-term mean, although within standard

deviation limits or not exceeding previous minimum-maximum values. An exception was January 2018, when runoff was the largest on the record, being more than twice as large (4.90 km^3 $month^{-1}$) as the long-term mean (2.25 km^3 $month^{-1}$). The maximum or close to the maximum value of monthly river runoff were also observed in September-December 2017. Thus, a larger than average river runoff in autumn-early winter 2017-2018 could cause slightly lower salinity in the gulf in spring 2018. However, a lower than average runoff in spring-summer 2018 could not strengthen the vertical stratification of the water column in late summer-autumn.

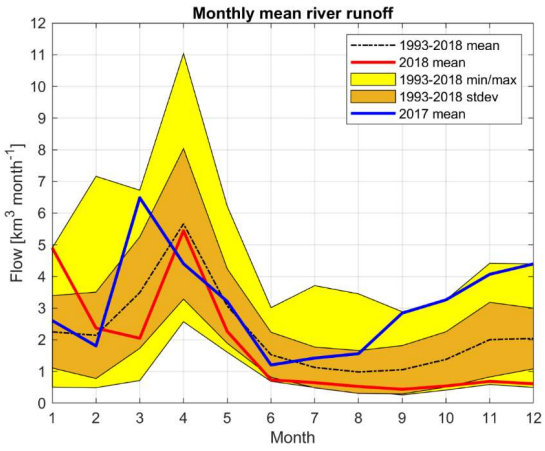

Figure 5. The course of mean monthly river runoff (dashed line), monthly minimum/maximum runoff (yellow area) and standard deviation (orange area) for 1993–2018. Bold red and blue lines mark monthly mean river runoff for the years 2018 and 2017, respectively.

3.2.3 Surface net solar radiation and air temperature

Based on ERA5 hourly surface net solar radiation data, we calculated the monthly mean net solar radiation and air temperature in 1979–2018 for the grid point close to station G1 (see Fig. 1 for location). The monthly mean net solar radiation in May 2018 was the highest during the observation period (Fig. 6a), and in June 2018, it was the third highest value after 1992 and 1979. Seasonal variation in air temperature in 2018 differed from the average (Fig. 6b). While air temperature in 2018 was lower than the average in February-March, a rapid increase of air temperature occurred in April-May, and it stayed higher than the monthly averages in 1979–2018 until October (Fig. 6b). Also, monthly mean air temperature in September 2018 was the highest of the observation period, and July and August 2018 were in the top 5 warmest years.

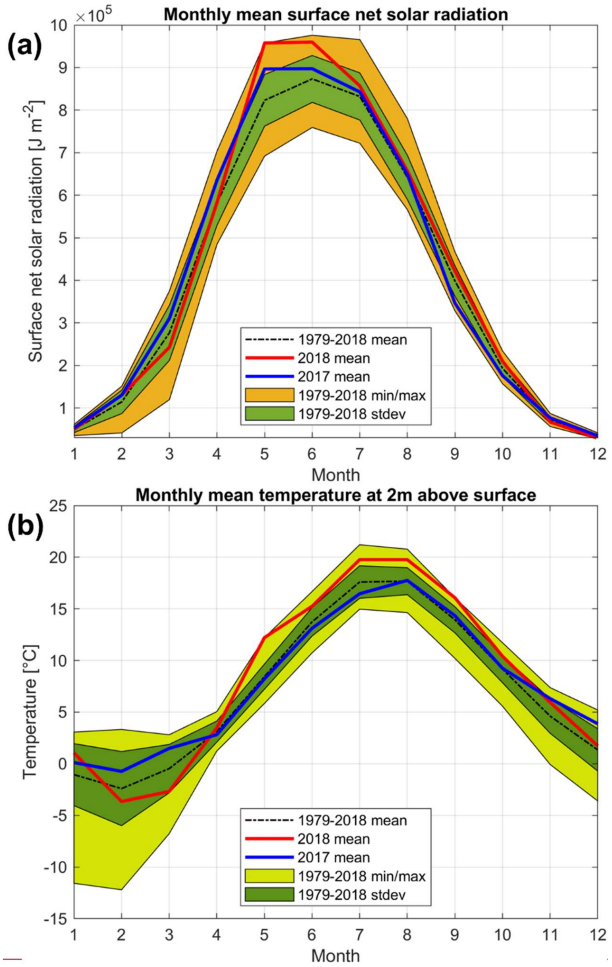

Figure 6. (a) Course of monthly mean surface net solar radiation (dashed line), monthly minimum/maximum (orange area), and standard deviation (green area) of radiation for the period 1979–2018 (ERA5 data). The bold red and blue lines mark monthly mean radiation for the year 2018 and 2017, respectively. (b) Course of monthly mean air temperature at 2 meters above surface (dashed line), monthly minimum/maximum (light green area), and standard deviation (darker green area) of

Formatted: Justified, Line spacing: 1.5 lines

temperature for the period 1979–2018 (ERA5 data). The bold red and blue lines mark monthly mean temperature for the year 2018 and 2017, respectively.

3.3. Deep layer dynamics and stratification

3.3.1. Oxygen, salinity and temperature sections through the Irbe Strait in 2018

For a qualitative description of probable links of the changes in the deep layer with the water exchange over the sill in the Irbe Strait, vertical sections of oxygen, salinity and temperature from the eastern Baltic Proper to the Gulf of Riga from May to August 2018 were constructed (Fig. 7). Based on the measurements at the end of May, the intrusion of saline water has reached Station 111 (near-bottom salinity was > 6.8 g kg^{-1}), while salinity was > 6.0 g kg^{-1} (up to 6.2 g kg^{-1}) in the near-bottom layer of deep areas of the gulf. Higher temperatures were associated with the saltier water in the near-bottom layer at Station 111, indicating that these waters could result from the mixing of gulf waters with the warmer surface waters from the Baltic Proper. Oxygen concentrations in the near-bottom layer in the central gulf and towards the Daugava river mouth in the southern gulf were at a level of 60% of saturation. Low temperatures of this near-bottom water mass suggest that it has been formed in winter or early spring as a mixture of local Gulf of Riga winter waters and saltier waters originating from the Baltic Proper. Higher salinity and lower oxygen content towards the Daugava river than in the Ruhnu Deep at the same depth could be related to the inclination of the boundary between the near-bottom and deep water due to atmospheric forcing and probably to more intense oxygen consumption at the sediment surface close to the mouths of major rivers.

In July, the deep area around monitoring station G1 was filled with higher salinity waters, > 6.4 g kg^{-1}, and oxygen concentrations had decreased to 40% of saturation (< 5 mg l^{-1}). Salinity in the near-bottom layer in the Irbe Strait was as high as in late May, but saltier waters' intrusion towards the central gulf was not so intense as during the previous survey. The measurements in late August suggest that the further filling of deeper areas with saline water continued between the surveys – salinity increased up to 6.55 g kg^{-1} at monitoring station G1. Hypoxic conditions with oxygen saturation below 20% were observed in the near-bottom layer of the central gulf. However, the salinity, temperature and oxygen distributions in the deep layers near the Irbe Strait area indicate that most probably outflow from the gulf prevailed below the seasonal thermocline at the end of August 2018.

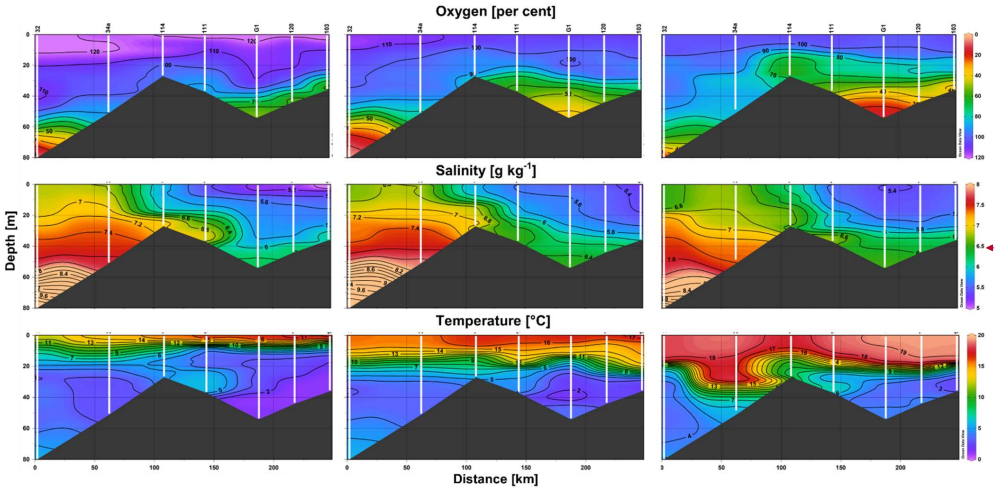

Formatted: Justified

Figure 7. Vertical sections of oxygen saturation (upper panels), salinity (center panels) and temperature (lower panels) on 30 May (left panels), 11 July (center panels) and 25-26 August (right panels) 2018 along the route from station 32 in the Baltic Proper through the Irbe Strait to station 103 in the Gulf of Riga (see the locations in Fig. 1).

Formatted: English (United States)

5

3.3.2. Comparative analysis of vertical distributions and wind forcing in 2017 and 2018

As described above, the most extensive hypoxia since 2005 was observed in the near-bottom layer of the central Gulf of Riga in 2018. The below analysis of the observed changes in vertical distributions and wind forcing was conducted, bearing in mind a suggestion that the 2018 hypoxia was likely related to the spreading of saline waters through the Irbe Strait (Fig. 7) that
10 created vertical stratification in the deep layer. To highlight the hypoxia-favorable conditions in 2018, the data from 2018 are compared with the respective data from 2017 that we chose as an example year when hypoxia did not develop. Also, as noted above, in 2017, monthly average winds did not display northerly winds that would support inflows.

Vertical profiles of temperature, salinity, density, and dissolved oxygen concentration in the Ruhnu Deep demonstrated
15 considerable differences between the years 2017 and 2018 (Fig. 8). By the end of May-early June 2017, the upper mixed layer was thick and relatively cold (9.7 °C), while in 2018, a thin and warm (up to 18.0 °C) near-surface layer formed (Fig. 8a and e). Though, near-bottom layer temperatures were <5 °C in both years. The surface layer was fresher in spring 2018 – salinity varied in April–May/June between 5.44 and 5.86 g kg^{-1} in 2017 and 5.14 and 5.65 g kg^{-1} in 2018. In 2017, near-bottom salinity variations were small, within the range of 5.90–6.06 g kg^{-1}, while in 2018, near-bottom salinity was higher and the changes

were larger than in 2017. Relatively high salinity was observed in the near-bottom layer already in April and salinity increased almost continuously from April to July 2018 from 6.06 to 6.50 g kg^{-1}, indicating the spreading of saltier waters into the Ruhnu Deep during that period.

The differences in vertical distributions of temperature and salinity in 2017 and 2018 were reflected in the water column stratification (Fig. 8c and g). The water column was well mixed at the end of April 2017. A single pycnocline with changing strength and thickness was observed between the upper mixed layer and the well-mixed deep layer throughout the summer 2017. In 2018, the situation was different – a pycnocline between the upper less saline water and saltier near-bottom water was observed below the 40 m depth in April. By the end of May 2018, two pycnoclines were formed, the deep pycnocline located below 35 m depth and the upper pycnocline (seasonal thermocline) at the 10 m depth. The intermediate layer (10–35 m) remained cold and well mixed. A relatively thin, practically mixed near-bottom layer was observed from May to October. The largest bottom to surface density difference was observed in August in both years – 2.05 kg m^{-3} in 2017 and 2.76 kg m^{-3} in 2018. Thus, vertical stratification was stronger in 2018.

Temporal courses of near-bottom oxygen concentrations in the Ruhnu Deep (Fig. 8d and h) showed clear decreasing trends from spring to autumn in 2017 and 2018. In 2018, oxygen concentration decreased simultaneously with the increase of NBL salinity until mid-July. From mid-July to the end of August, near-bottom salinity increased only slightly but hypoxia developed in the near-bottom layer. The signs of vertical mixing, as an expansion of the near-bottom layer and a decrease in salinity, are apparent when comparing the vertical profiles from August and October 2018. However, hypoxic conditions with no decrease in oxygen concentration prevailed until the end of October 2018. In summer–autumn 2017, the NBL salinity only slightly increased, and hypoxia was not observed.

A prominent feature in the Ruhnu Deep in 2018 was the haline stratification in the deep layer, potentially restricting mixing between the near-bottom layer and the water column above. The spreading of saltier waters from the eastern Baltic Proper to the Gulf of Riga over the Irbe Strait sill was demonstrated by the vertical sections of salinity (Fig. 7). The time series of along-coast component (NNE–SSW) of wind stress revealed the periods in both years, 2017 and 2018, when the upwelling-favorable winds with negative wind stress τ_N exceeding –0.2 N m^{-2} occurred, supporting the inflows into the near-bottom layer of the central gulf (Fig. 9). However, the main difference between these two years is expressed by the cumulative wind stress, which followed the long-term pattern in 2017 but clearly deviated from it in 2018. From February to the end of July in 2018, wind forcing, on average, supported the inflow of saltier waters into the Gulf of Riga, as revealed by the decrease in the cumulative wind stress (Fig. 9). From the beginning of August, the winds from opposite direction, which could cause downwelling along the eastern coast of the Baltic Proper, prevailed. Thus, the inflows of sub-thermocline waters into the Gulf of Riga could have been blocked in late summer 2018.

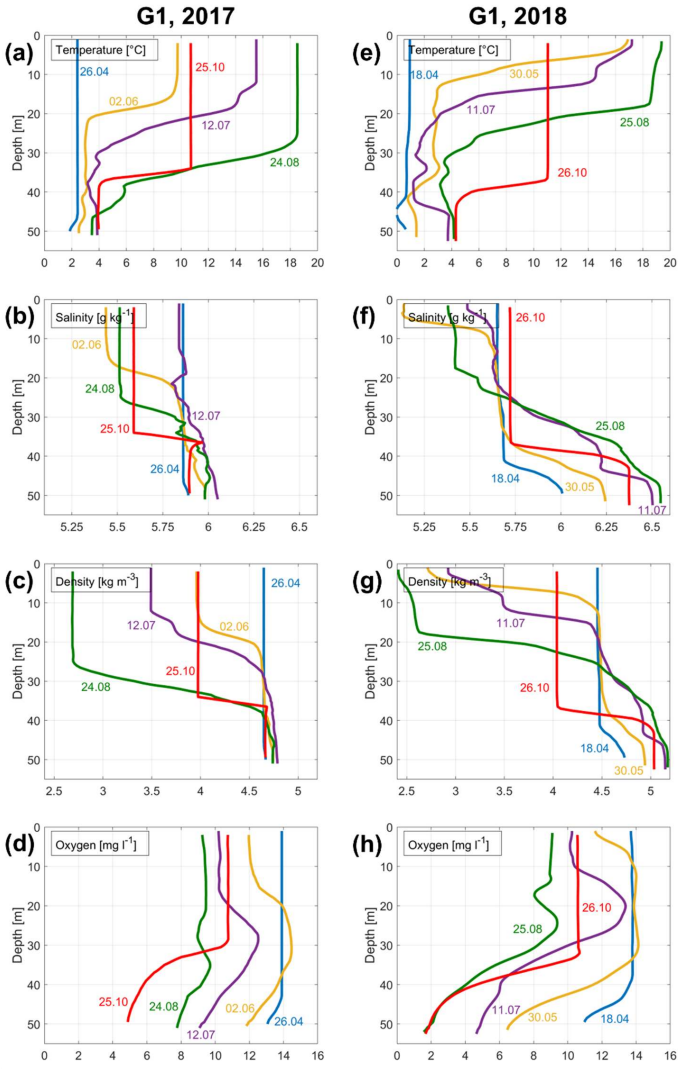

Figure 8. Vertical profiles of temperature (a, e), salinity (b, f), density anomaly (c, g), and dissolved oxygen concentration (d, h) measured in the Ruhnu Deep (station G1, see location in Fig. 1) in 2017 (left panels) and 2018 (right panels).

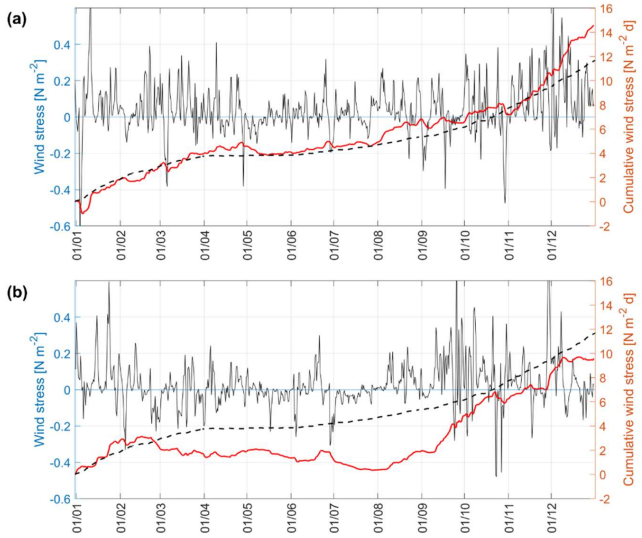

Figure 9. Time series of local along-coast (NNE–SSW) component of wind stress τ_N (black line, positive northward), cumulative wind stress (red line) in 2017 (a) and 2018 (b) (6h moving average is shown) and cumulative wind stress based on mean wind stress for 1979–2018 from 1 January to 31 December. See the location of the ERA5 grid point in the EGB close to the Irbe Strait in Fig. 1.

3.4. High-frequency dynamics of temperature, salinity, and dissolved oxygen in relation to the wind forcing

High-frequency measurements with the buoy profiler were carried out from 5 to 21 August 2018 close to station G1 (see Fig. 1). Time series of the vertical distributions of temperature, salinity and oxygen together with the wind speed variability are presented in Fig. 10. Two strong wind events passed the Gulf of Riga on 10 and 12 August, when the average wind speed was up to 11.3 and 13.6 m s^{-1}, respectively. The first wind pulse slightly changed the upper mixed layer depth. Although the thickness of the hypoxic, saltier layer slightly increased after the first wind event, the variability of salinity and oxygen concentration in the near-bottom layer was small until the second wind event. The second wind pulse on 12 August caused a rapid deepening of the thermocline and an increase of the upper mixed layer depth by about 8 m. Near-bottom layer salinity and thickness increased during the wind pulse. At the same time, the oxygen concentration remained approximately on the same level, but the thickness of the hypoxic layer increased about 8 m. The wind speed decreased on 13 August and remained low (< 5 m s^{-1}) until 17 August. The decrease of wind speed was accompanied by the decrease of salinity and increase of

oxygen concentration over the hypoxia threshold in the near-bottom layer until the noon of 15 August. A rapid increase of salinity and decrease of oxygen concentration occurred in the second half of 15 August. A relatively thick hypoxic layer remained at the measurement site until 18 August. Further, until the end of measurements, the decreasing trend of hypoxic layer thickness and salinity was observed, gradually approaching conditions similar to the beginning of the measurements. To conclude, the buoy profiler measurements displayed high variability of the upper mixed layer temperature and depth caused by wind-induced mixing.

High variability of near-bottom layer salinity and oxygen concentration and thickness of the near-bottom haline hypoxic layer, in the time scale of few days, was most probably caused by the wind forced advection, not vertical mixing between the NBL and the water layer above it. Deepest measured oxygen concentrations varied from 1.3 to 3.3 mg l-1, with the mean of 2.1 mg l-1, when taking into account profiles with the maximum depth of ≥ 50 m. The standard deviation of the deepest oxygen measurements was 0.50 mg l-1, and the coefficient of variation 24 %. These statistical parameters give an estimate of the uncertainty in using near-bottom oxygen values from a single measurement that should represent a two-week period (when the monitoring is conducted with a time step of two weeks). The uncertainty is higher for the current monitoring program with a sampling step of 1.5-2 months.

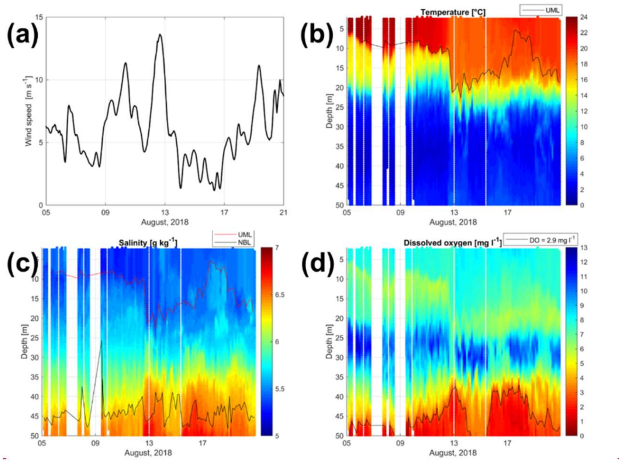

Figure 10. Time series of wind speed (ERA-5; 5h moving average) at the location close to the buoy station (a) and vertical distribution of (b) temperature, (c) salinity and (d) dissolved oxygen measured at the buoy station from 5 to 21 August 2018. DO = 2.9 mg l^{-1} marks the hypoxia threshold. UML is the upper mixed layer and NBL is the near-bottom mixed layer, both defined as described in Sect. 2.

~~1.1. 3.5. Estimates of oxygen consumption and sediment release of phosphates~~

~~Oxygen consumption was estimated using Eqs. 1 and 2, based on the changes in salinity and oxygen concentration in the near-bottom mixed layer in the Ruhnu Deep and the Irbe Strait. A comparison of the measured salinity changes and estimated changes in the NBL due to diffusion shows that the salt flux due to advection and lateral mixing had about three times larger contribution to the salinity changes than vertical diffusion (Table 1; row "$Sal^{t2}(G1) - Sal^{t1}(G1)$ due to diffusion (g kg^{-1})") from mid-April to mid-July while it was only slightly larger from mid-July until the end of August 2018. Both advection and vertical diffusion should increase the oxygen concentration in the gulf NBL and had comparable contributions varying from 0.67 mg l^{-1} to 1.74 mg l^{-1} and 0.75 mg l^{-1} to 1.46 mg l^{-1}, respectively, for studied three periods (Table 1). Advection and lateral mixing had the largest influence on the oxygen content when the difference between the NBL oxygen concentrations between the central gulf and the Irbe Strait was the largest. However, the measurements and calculations according to the introduced approach show that oxygen consumption had to be large enough to exhaust oxygen brought by advection and diffusion and cause further oxygen depletion in the NBL. The estimates of the consumption rate per unit bottom area, which could be a more relevant indicator for oxygen consumption as opposed to oxygen depletion per volume unit of the NBL, assuming that oxygen consumption takes mostly place on the sediment surface, varied from 1.53 to 1.75 mmol m^{-2} h^{-1} in 2018 (Table 1; row "DO consumption rate per unit bottom area").~~

~~We also assessed consumption rates from August to October in 2018, but the prevailing conditions (outflow from GoR through the Irbe Strait) were unsuitable for applying the method. We have assumed an inflow of oxygenated EGB sub-thermocline waters through the Irbe Strait to deeper areas of the GoR. Secondly, a stable stratification of the water column, which hinders vertical mixing between the NBL and the water layer above, should exist to apply the gradient method of diffusion flux estimates. For instance, in spring 2017, the near-bottom layer was not separated by a vertical density gradient from the layers above. Thus, the gradient method of estimating vertical salt and oxygen flux is not applicable. Also, oxygen concentrations in the NBL of the Irbe Strait were similar or even lower than the oxygen concentration at station G1 in 2017, probably due to prevailing outflows of deep GoR waters through the Irbe Strait.~~

Formatted: Outline numbered + Level: 2 + Numbering Style: 1, 2, 3, … + Start at: 1 + Alignment: Left + Aligned at: 0.63 cm + Indent at: 1.4 cm

Formatted: English (United States)

Table 1. Estimated changes in NBL salinity and oxygen concentration due to advection and diffusion and estimated consumption rates between the monitoring campaigns in 2018. Parameters measured in or estimated for monitoring campaigns' start/end are denoted by t1/t2. Sal marks salinity, DO marks dissolved oxygen and NBL marks near-bottom mixed layer.

Period start (t1)	18.04.2018	30.05.2018	11.07.2018
Period end (t2)	30.05.2018	11.07.2018	25.08.2018
$Sal^{t1}(114)$ (g kg^{-1})	6.77	7.17	7.27
$Sal^{t1}(G1)$ (g kg^{-1})	5.99	6.22	6.48
$Sal^{t2}(G1)$ (g kg^{-1})	6.22	6.48	6.51
$Sal^{t2}(G1) - Sal^{t1}(G1)$ due to diffusion (g kg^{-1})	-0.14	-0.13	-0.11
$O_2^{t1}(114)$ (mg l^{-1})	13.42	12.46	11.08
$O_2^{t1}(G1)$ (mg l^{-1})	12.01	8.27	5.16
$O_2^{t2m}(G1)$ (measured, mg l^{-1})	8.27	5.16	2.52
$O_2^{t2}(G1)$ estimated due to advection and lateral mixing (mg l^{-1})	12.68	10.01	6.18
$O_2^{t2}(G1) - O_2^{t1}(G1)$ due to advection and lateral mixing (mg l^{-1})	0.67	1.74	1.02
$O_2^{t2}(G1) - O_2^{t1}(G1)$ due to diffusion (mg l^{-1})	1.46	1.09	0.75
NBL thickness (m)	9.5	9.5	12.0
DO consumption rate per unit bottom area (mmol O_2 m^{-2} h^{-1})	**1.72**	**1.75**	**1.53**

In 2018, hypoxic conditions were observed at station G1 and with the developing oxygen depletion, phosphate concentrations increased in the near-bottom layer (Fig. 11). However, note that the phosphate concentrations were already elevated in July when the near-bottom oxygen values (2-3 m from the seabed) did not indicate hypoxic conditions there yet. Still, hypoxia could be the case at the sediment-water interface. The amount of phosphates released from sediments was estimated using the same approach as for oxygen consumption (see Sect. 2), taking into account the concentrations in the near-bottom layer at stations G1 and 114 – the latter representing the inflowing water. Since the vertical resolution of sampling was scarce (step was 10 m), we used only the deepest measured phosphate concentration as the value characterizing the entire NBL, and the vertical gradient was estimated between the phosphate concentrations at 50-52 m the deepest sampling point and 4010-12 m. above it.

3. Results

3.1. Inter-annual variability of dissolved oxygen in the near-bottom layer

We characterized the long-term development of oxygen conditions in the Gulf of Riga using near-bottom oxygen measurements at the deepest stations G1 and 121 (bottom depth 54 m) and yearly average late summer (August) and autumn (October-November) near-bottom oxygen concentrations at all stations with depth >= 40 m (see station locations in Fig. 1). Based on the data obtained from the deepest stations, late summer-autumn hypoxia occurred in about 50% of years in 2005–2018 (Fig. 2). No hypoxia was observed in 2006–2011, except for one value close to 2.9 mg l^{-1} in 2009, but note low sampling frequency. Hypoxic conditions have been recorded every year since 2012, with the exception of in 2016 and 2017. Based on the data from all monitoring stations from 2005-2018, no trend in the deep layer oxygen concentrations was detected in summer, but a statistically significant ($p < 0.05$) trend at a rate of 0.45 mg l^{-1} $year^{-1}$ was found in autumn ($R^2 = 0.50$, $n = 13$). Thus, the monitoring data suggest that the hypoxic conditions observed in 2018 are – in general – in line with the long-term trend.

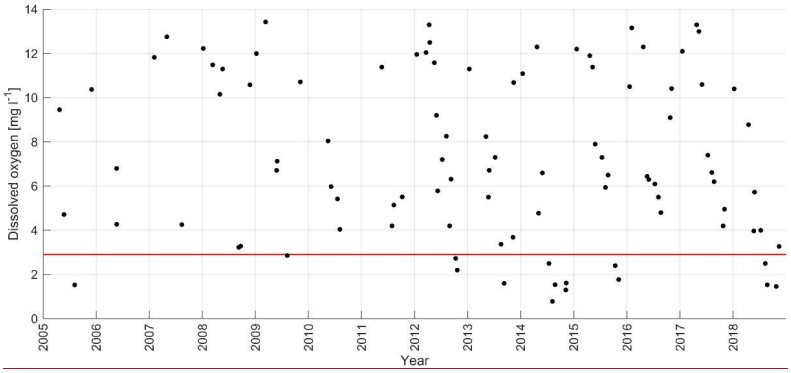

Figure 2. Inter-annual variability of near-bottom dissolved oxygen concentration at monitoring stations G1 and 121 in 2005–2018. The ~~changes in~~ red line denotes the oxygen concentration 2.9 mg l^{-1} (threshold concentration for hypoxia).

We studied the links between the long-term trend and variability of near-bottom oxygen and other environmental parameters, such as salinity and nutrient concentrations. No significant trend in near-bottom salinity was revealed in 2005-2018. Using simultaneously measured near-bottom salinity and oxygen values at station G1 from August to November in 2005-2018, we found a statistically significant ($R^2 = 0.24$, $n = 36$, $p < 0.05$) negative relationship – low oxygen concentrations corresponded

Formatted: Outline numbered + Level: 1 + Numbering Style: 1, 2, 3, … + Start at: 1 + Alignment: Left + Aligned at: 0 cm + Indent at: 0.63 cm

to high salinity values. However, there are examples where hypoxia occurred at salinities 5.8 g kg^{-1} (in 2012 and 2015) and did not exist at 6.5 g kg^{-1} (in 2010).

The analysis of near-bottom phosphate concentrations at stations with depth >= 40 m revealed a statistically significant increase in concentrations in late summer (0.08 µM $year^{-1}$, R^2 = 0.47, n = 14) and autumn (0.12 µM $year^{-1}$, R^2 = 0.34, n = 13). A statistically significant negative correlation was obtained between the deep layer oxygen and phosphate concentrations in autumn (R^2 = 0.79, n = 13, $p<0.05$). The near-bottom layer oxygen in autumn also significantly correlated with the next year winter (January) phosphate concentration in the entire water column (R^2 = 0.45, n = 9, $p<0.05$). Thus, the impact of the hypoxia deepening is also seen in the trends of phosphate concentrations.

3.2. Seasonal and inter-annual variability in the vertical distribution

Based on the vertical profiles of dissolved oxygen collected on an at least bi-monthly basis in 2012-2018, a clear seasonal pattern is apparent at all depths, with the largest amplitude occurring in the near-bottom layer (Fig. 3a). The lowest oxygen concentrations were measured in late summer/autumn, but the oxygen levels did not always drop below the hypoxia threshold (as in 2016 and 2017). The deepest minima were observed in 2014 (0.8 mg l^{-1}) and 2018 (1.5 mg l^{-1}). As pointed out above, hypoxia was observed in 2012-2015 and 2018, but the duration and vertical extent of hypoxia differed between the years (Fig. 3a, Table 1). The seasonal hypoxia was first detected in July in the year 2014, August in 2018, September in 2013, and October in 2012 and 2015. The upper border of the hypoxic layer was at its shallowest depth in 2018 (45.0 m). Accordingly, the estimated spatial extent of hypoxia was the largest in 2018, when the hypoxic waters covered 5.2% (830 km^2) of the gulf's bottom area. In the other years with hypoxia (2012-2015), the estimates of the bottom area covered by hypoxic waters did not differ greatly, varying between 2.1% and 2.7% (340-430 km^2).

Seasonal patterns also dominate the variability of vertical distributions of temperature, salinity and density anomaly (Fig. 3b-d), but certain inter-annual differences in water column parameters can be noticed (Table 1). The observed UML temperature maxima were higher in the summers of 2014 and 2018. Lower summer UML salinities (≤5.2 g kg^{-1}) were observed in 2012, 2013, and 2018, and increased NBL salinity values (≥ 6.5 g kg^{-1}) were registered in the summers of 2013 and 2018. The largest density differences between the bottom and surface layer, 3.4 kg m^{-3} and 3.5 kg m^{-3} – which are mostly associated with high UML temperatures – were found in 2014 and 2018. High NBL salinity and low UML salinity contributed to the observed relatively strong water column stratification in 2013 (the third-strongest stratification in 2012-2018), although the summer UML temperature remained low in 2013 (Table 1). The weakest vertical stratification was observed in 2017, when the density difference between the NBL and UML was close to 2.0 kg m^{-3}.

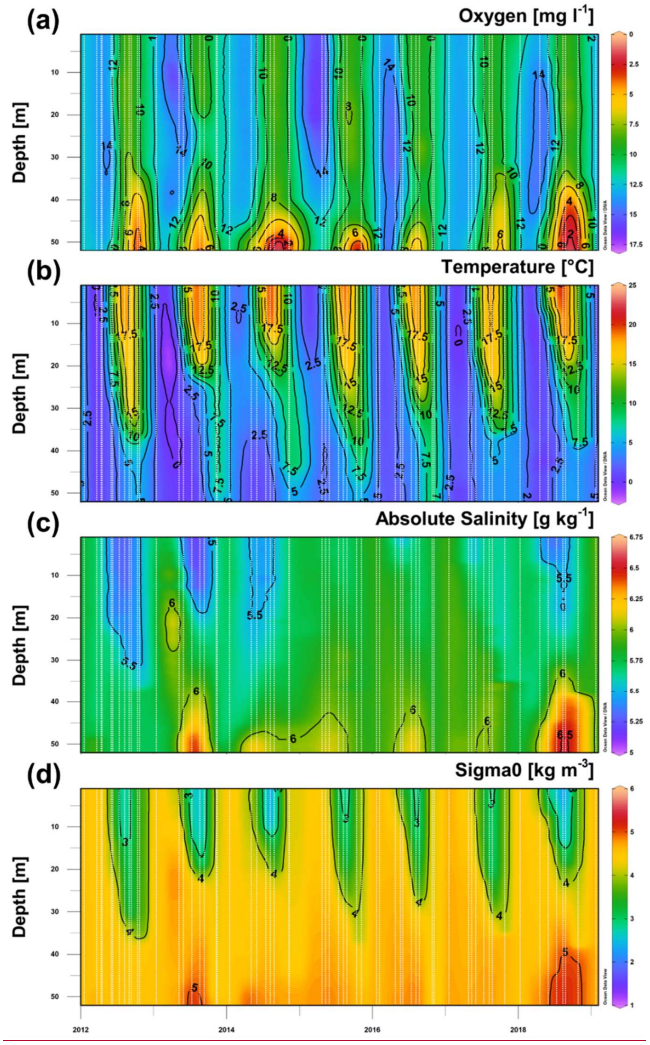

Figure 3. Time series of the vertical distribution of oxygen concentration (a), temperature (b), salinity (c), and density anomaly (d) at stations G1 and 121 in 2012-2018 (including January 2019). Vertical white dashed lines mark the time of measured profiles.

Thus, the years with strong stratification (2013, 2014 and 2018; Table 1) related to high UML temperature, low UML salinity, and high NBL salinity were among those with near-bottom hypoxia. In 2017, the stratification was the weakest, and hypoxia did not develop. Still, the density difference between the NBL and UML was weaker in 2012 and 2015 than in 2016 – but in 2012 and 2015, hypoxia was observed, whereas in 2016, it was not. We suggest that vertical stratification is the key factor that influences the development of hypoxia, but the overall stratification of the water column alone does not explain the occurrence, duration, and spatial extent of hypoxia. A further, more detailed analysis of water column stratification is presented in Sect. 3.4 together with the description of meteorological and hydrological forcing data.

Table 1. Characteristics of seasonal hypoxia and stratification parameters in the Gulf of Riga in 2012-2018, based on CTD profiles from May to November at stations G1 and 121. Observed maxima of UML temperature, NBL salinity, and density difference between NBL and UML and minima of UML salinity are given.

Year	Earliest hypoxia detection month	Min. depth of hypoxia m	Max. hypoxic area % (km^2)	UML max temperature °C	UML min salinity g kg^{-1}	NBL max salinity g kg^{-1}	NBL-UML density kg m^{-3}
2012	October	48.5	2.7 (430)	18.97	5.16	5.77	2.20
2013	September	49.0	2.4 (380)	18.59	5.21	6.51	2.72
2014	July	49.0	2.4 (380)	23.46	5.28	6.08	3.38
2015	October	49.5	2.1 (340)	19.41	5.65	5.82	2.22
2016	-	-	-	19.37	5.38	6.21	2.35
2017	-	-	-	18.50	5.26	6.01	2.05
2018	August	45.0	5.2 (830)	22.36	5.17	6.51	3.46

3.3. Temporal ~~due to advection and lateral~~ development of hypoxia in 2018

To demonstrate the development of hypoxia and vertical stratification in 2018 in more detail and to compare it with that of the year without hypoxia, we present vertical profiles of temperature, salinity, density, and dissolved oxygen concentration in the Ruhnu Deep in 2017 and 2018 (Fig. 4). A major difference between the years is evident in a much faster decrease of near-bottom oxygen concentrations in spring 2018 than in 2017. This could be related to the differences in vertical stratification in the springs of these two years. Salinity stratification in the deep layer was already established in the middle of April 2018, and two pycnoclines were formed by the end of May 2018. The water column was well mixed at the end of April 2017, and although the seasonal thermocline developed by the end of May, neither the saltier near-bottom waters nor the deep pycnocline was observed in summer 2017. We suggest that the deep layer stratification influenced the near-bottom oxygen depletion in the gulf in spring-summer 2018 by restricting mixing between the near-bottom layer and the water column above.

The formation of the saltier near-bottom layer and the deep stratification in a sea basin separated from the open sea by a sill must be related to the inflow of saltier and denser waters from the open sea. The spreading of waters from the eastern Baltic Proper to the Gulf of Riga over the Irbe Strait sill can be demonstrated by the vertical sections of oxygen, salinity, and temperature (Fig. 5). Based on the measurements at the end of May, the intrusion of saltier waters over the sill is evident up to station 111. Higher temperatures associated with the saltier water in the near-bottom layer at station 111 could indicate the mixing of gulf waters with the warmer waters from the Baltic Proper. Oxygen concentrations in the near-bottom layer in the central gulf and towards the Daugava river mouth in the southern gulf were at a level of 60% saturation. Low temperatures of this near-bottom water mass suggest that it had been formed in winter or early spring as a mixture of local Gulf of Riga winter waters and saltier waters originating from the Baltic Proper.

In July, the deep area around monitoring station G1 was filled with saltier waters, and oxygen concentrations had decreased to 40% of saturation (< 5 mg l^{-1}). The measurements in late August suggest that the further filling of deeper areas with saline water continued between the surveys – salinity increased at all deeper monitoring stations. We also point to an increase of salinity in the water layer of 35-45 m, which is well seen on the consecutive profiles measured in July and August at station G1 (Fig. 4). This could be related to the inflow of denser waters in July-August that moved the "old" near-bottom waters upwards. Hypoxic conditions with oxygen saturation below 20% were observed in the near-bottom layer of the central gulf. However, the salinity, temperature, and oxygen distributions in the deep layers near the Irbe Strait indicate that outflow from the gulf likely prevailed below the seasonal thermocline at the end of August 2018 (Fig. 5 lower panel).

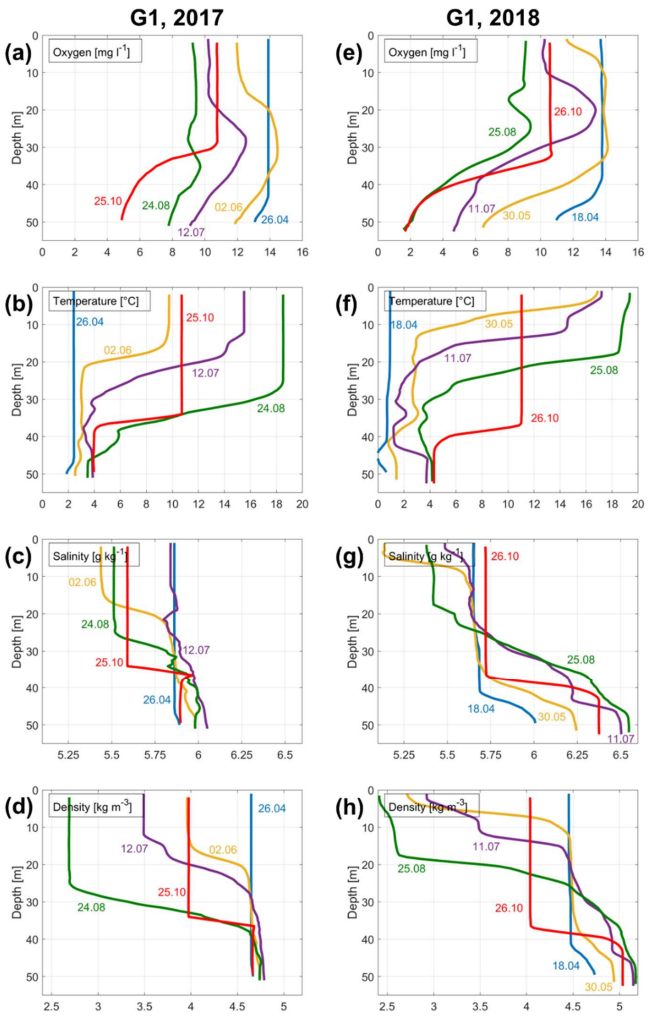

Figure 4. Vertical profiles of dissolved oxygen concentration (a, e), temperature (b, f), salinity (c, g), and density anomaly (d, h) measured in the Ruhnu Deep (station G1, see location in Fig. 1) in 2017 (left panels) and 2018 (right panels).

Formatted: English (United States)

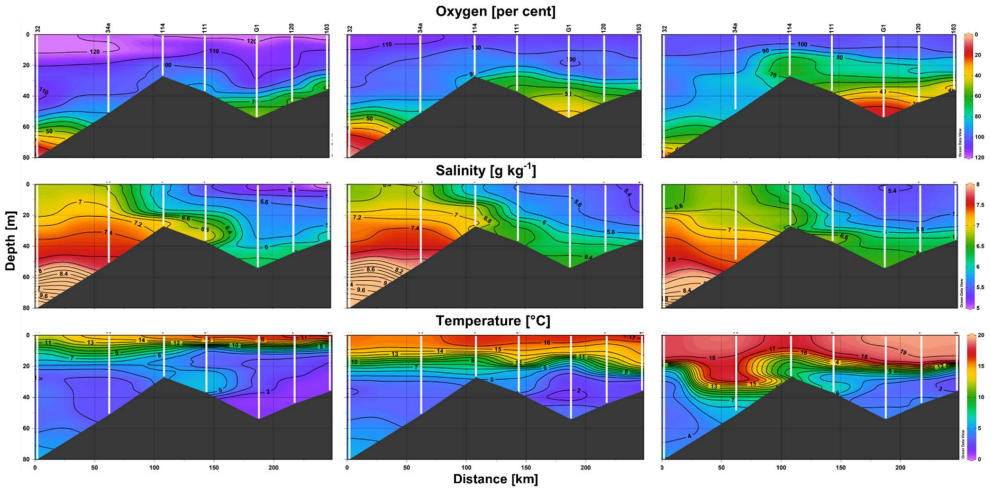

Figure 5. Vertical sections of oxygen saturation (upper panels), salinity (center panels), and temperature (lower panels) on 30 May (left panels), 11 July (center panels), and 25-26 August (right panels) 2018 along the route from station 32 in the Baltic Proper through the Irbe Strait to station 103 near Daugava river mouth in the Gulf of Riga (see the locations in Fig. 1).

3.4. Analysis of meteorological and hydrological conditions

The above analysis showed that vertical stratification is a major factor influencing the development of near-bottom hypoxia in the Gulf of Riga. Strong stratification could be related to high surface radiation and weak winds, as well as large river runoff and the inflow of saltier waters into the near-bottom layer. Solar radiation in 2018 was higher than that of the long-term average for all months from spring to autumn, with the highest monthly mean value during the observation period being in 2018 in May (Fig. 6a). Seasonal variation of air temperature in 2018 differed from the average, as well, with a rapid increase in April-May and higher monthly mean values than the long-term averages until October (Fig. 6b). Monthly mean air temperatures in July-September 2018 were in the top of 5 warmest years in 1979-2018. The monthly average wind speed from February to August was lower in 2018 than the long-term mean for the respective month, except in April (Fig. 6c). The lowest wind speed for May in 1979-2018 was found in 2018, suggesting that the wind-induced mixing of the water column in May was the weakest in 2018, if compared with that of the other years. Thus, both the high heat flux and low mixing intensity supported the development of a strong stratification in 2018. At the same time, solar radiation, air temperature, and wind speed in 2017

were mostly close to the long-term averages – except the low wind speed in May and the high wind speed in June 2017 (Figs. 6a-c).

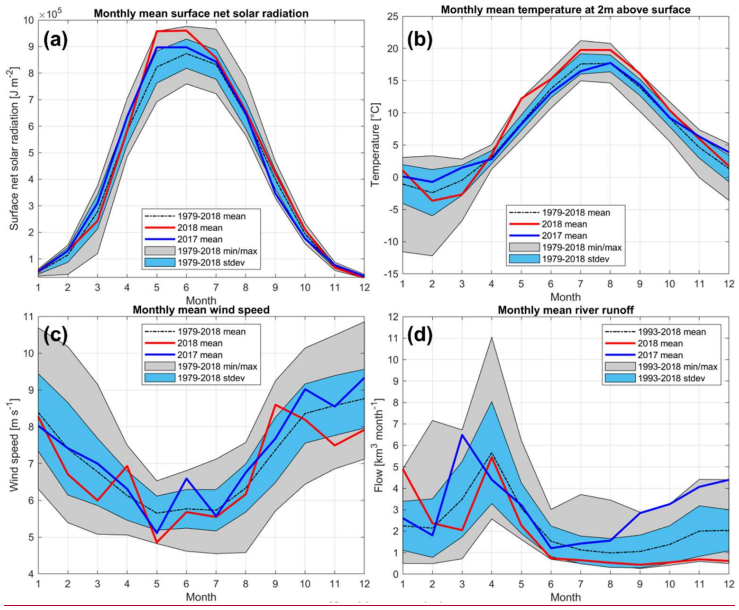

Formatted: Justified, Line spacing: 1.5 lines

Figure 6. Courses of monthly mean, minimum/maximum and standard deviation of (a) surface radiation, (b) air temperature, and (c) wind speed for the period of 1979–2018, and (d) river runoff for the period of 1993–2018. The monthly mean values of listed parameters for 2017 and 2018 are shown as blue and red lines, respectively. For meteorological parameters, ERA5 data are used from the central Gulf of Riga (see the location of the grid cell in Fig. 1).

A comparison of monthly river runoff values from 2018 with the long-term mean values (1993–2018) shows that the 2018 runoff was mostly lower than the long-term mean – although within standard deviation limits (Fig. 6d). An exception was found in January 2018, when runoff was the largest on the record, being more than twice as large (4.90 km^3 month^{-1}) as the long-term mean (2.25 km^3 month^{-1}). The maximum or close to the maximum value of monthly river runoff was also observed in September-December 2017. A larger than average river runoff in autumn-early winter 2017-2018 could result in fresher surface waters, stronger vertical stratification, and larger nutrient and organic matter load to the Gulf of Riga.

The development of vertical stratification characterized by potential energy anomaly estimated using meteorological and river runoff data (Fig. 7) in general reflects the same differences between the years as the simple comparison of temperature, salinity and density in the UML and NBL (Table 1). The strongest stratification is predicted for summers 2013 and 2018, and strong stratification was characteristic for summer 2014, based on both the estimates using meteorological and runoff data and CTD profiles. The years 2012, 2015 and 2017 are among the years with the weakest stratification. However, very strong stratification is also predicted for 2016, which was not captured by the CTD measurements (note the high variability and the measurement step of about 1-2 months). Another relatively large discrepancy between the prediction and CTD based estimates of PEA is seen for autumn 2013 – the prediction based on meteorological and hydrological data revealed a much longer stratified period than the measurements. This year was remarkable, with the largest river runoff and relatively high temperatures in autumn. When analyzing the contribution of the three components in Eq. 1, the biggest influence comes from the warming and development of seasonal thermocline in spring and wind-induced mixing together with negative heat flux in autumn. River runoff had, in general, lower contribution to the development of stratification, although it is visible in early spring 2013 (Fig. 7).

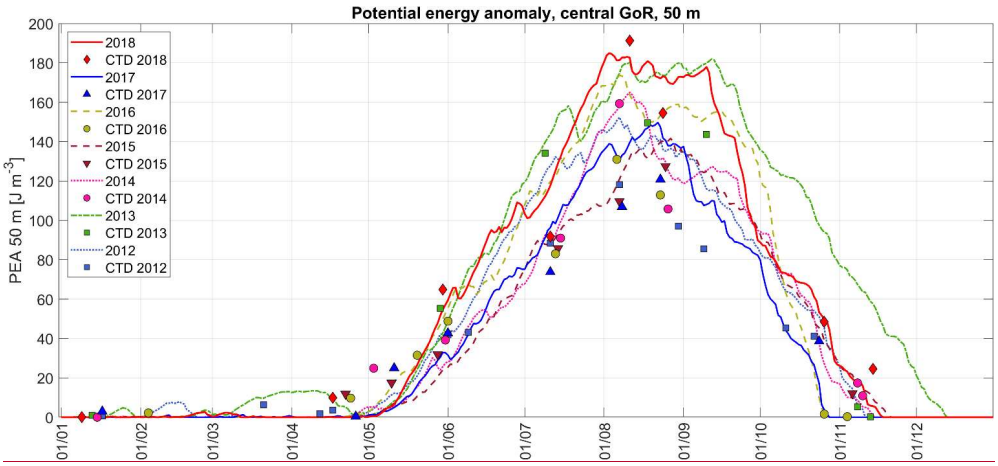

Figure 7. Changes in vertical stratification (potential energy anomaly, PEA, characterizing energy needed to mix the water column fully) in the central Gulf of Riga in 20012-2018 based on CTD profiles (markers) and estimated using meteorological (ERA5 data are from the central Gulf of Riga) and river runoff data (curves; the methods are presented in Sect. 2).

Formatted: Justified

Formatted: English (United States)

The fastest development of stratification in 2013 and 2018 is well seen in both the prediction and CTD measurements. The other years with stronger stratification in early summer were 2012 and 2016. A critical difference between the years can also be noticed in the stratification decay in autumn. The earliest disappearance of vertical stratification is predicted for 2016 and 2017 – the water column was fully mixed by the end of October. In comparison, the water column was fully mixed remarkably later in 2015 – in the second half of November. It could be why hypoxia was detected in late October and early November 2015 but was not observed in late October 2016 and 2017. We cannot prove whether hypoxia occurred in 2016 and 2017 since no data were available from late August to late October. However, the prolonged existence of stratification in autumn is one of the factors increasing the probability of the appearance of near-bottom hypoxia.

The analysis of the time series of along-coast component (NNE–SSW) of wind stress supports the described inflow-outflow suggestions for 2018 (see Sect. 3.3). Upwelling-favorable winds with negative wind stress τ_{NNE} exceeding –0.2 N m^{-2} that could be related to the inflows of saltier waters into the Gulf of Riga were observed in February-March, May, early June and late June 2018 (Fig. 8a). A major deviation from the long-term pattern is also evident in cumulative wind stress in 2018 – wind forcing from February to the end of July supported the near-bottom inflows (seen as the decrease in the cumulative wind stress; Fig. 8a). From the beginning of August, the winds from the opposite direction – which could cause downwelling along the eastern coast of the Baltic Proper – prevailed. Thus, the inflows of sub-thermocline waters into the Gulf of Riga could have been blocked in late summer 2018, as also seen in Fig. 5 demonstrating the outflow of gulf deep layer waters to the Irbe Strait at the end of August.

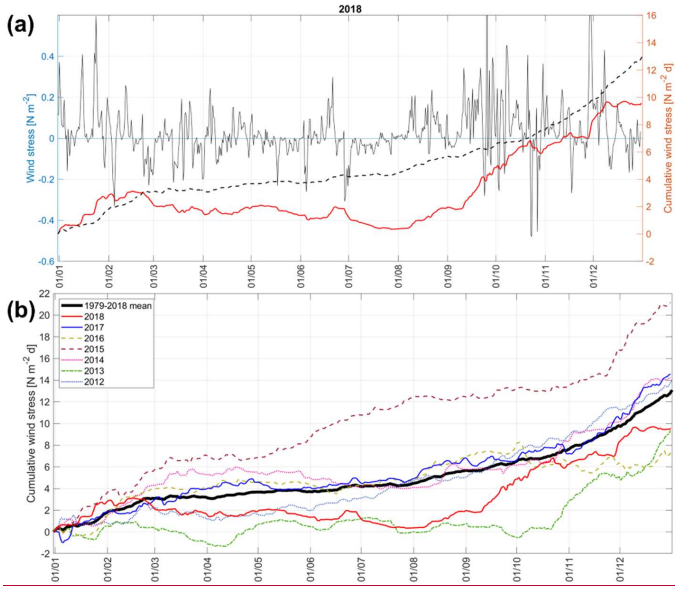

Figure 8. (a) Time series of along-coast (NNE–SSW) component of wind stress τ_{NNE} and cumulative wind stress in 2018 (6h moving average is shown). (b) Cumulative wind stress for each year in 2012-2018. Average cumulative wind stress curve for 1979-2018 is shown in both panels. Data were extracted from the ERA5 grid point outside the gulf (see location in Fig. 1).

Similar to 2018, the cumulative wind stress in 2013 largely deviated from the long-term mean (Fig. 8b). The inflow-favorable winds dominated in spring-summer, supporting the development of vertical stratification in the gulf deep layer. Although these inflows potentially brought more oxygen to the NBL, hypoxia developed in late summer both years, probably due to high consumption of oxygen and enhanced stratification restricting vertical mixing. A significant difference between these two years appeared in September – in 2013, the inflow-favorable winds persisted, while in 2018, the winds from opposite directions started to prevail. This difference could be a reason for an earlier disappearance of hypoxia in 2013, since further inflows could bring enough oxygen to the NBL this year. Inflow supporting wind conditions were also observed in late spring-summer 2014, forming a relatively thin NBL (with its boundary at 46 m), and hypoxia appeared already in July 2014. Almost no inflow supporting winds occurred in 2015, and probably no additional oxygen reached the gulf central area from the Irbe Strait. Although stratification was not strong and the NBL salinity was low this year (see Table 1), hypoxia developed in 2015, but later – in late October in 2015, while hypoxia in the other years was observed in July-September (Figs. 2 and 3). Cumulative wind stress graphs generally followed the long-term mean in 2016 and 2017 (Fig. 8b), and in these years, no hypoxia was

observed. We can conclude that in the case of meteorological conditions corresponding to the 1979-2018 average conditions, the probability of the development of near-bottom hypoxia is not high in the Gulf of Riga.

3.5. Estimates of oxygen consumption and sediment release of phosphates

~~water and "new" inflowing water and~~ We estimated fluxes of dissolved oxygen to the NBL at station G1 in summer 2018 due to vertical diffusion ~~were estimated using Eqs. 1~~ and ~~2~~lateral advection and mixing. Based on the gradient method~~. As seen from Table 2~~, (Eqs. 4-5), the estimated vertical diffusive flux varied between 0.26 and 0.43 mmol O_2 m^{-2} h^{-1}, corresponding to the changes in NBL oxygen concentration from 0.50 to 1.05 mg l^{-1} $month^{-1}$ (Table 2). When converting the vertical fluxes per unit area into the changes in concentration, the average thickness of the NBL in the period under consideration was taken into account. The estimated changes in oxygen concentration due to advection (Eq. 6) had comparable values, varying from 0.48 to 1.24 mg l^{-1} $month^{-1}$. According to the measurements, the NBL oxygen concentration continuously decreased in summer 2018, showing that oxygen consumption had to be large enough to exhaust oxygen brought by diffusion and advection, and cause further oxygen depletion in the NBL. We found that consumption could cause oxygen depletion in the NBL by 2.94–4.24 mg l^{-1} $month^{-1}$ or, in total, by 16.2 mg l^{-1} from mid-April to late-August 2018 (Eq. 7). The estimated consumption rate per unit bottom area (Eq. 8) varied from 1.53 to 1.75 mmol O_2 m^{-2} h^{-1} in 2018. The relative variation of the latter was smaller than for depletion, since, assuming that consumption mainly takes place at the sediment surface, the same consumption rate leads to stronger depletion in the case of a thinner NBL.

Table 2. Estimated changes in NBL salinity and oxygen concentration due to advection and diffusion (presented as the changes per month to ease the comparison between the periods) and estimated consumption rates from mid-April to late August 2018.

Period start (t1) and end (t2)		18.04-30.05	30.05-11.07	11.07-25.08
$O_2^{t1}(114)$	mg l^{-1}	13.42	12.46	11.08
$O_2^{t1}(G1)$	mg l^{-1}	12.01	8.27	5.16
$O_2^{t2m}(G1)$	mg l^{-1}	8.27	5.16	2.52
Measured O_2 depletion at G1	mg l^{-1} $month^{-1}$	2.67	2.22	1.76
$Sal^{t1}(114)$	g kg^{-1}	6.77	7.17	7.27
$Sal^{t1}(G1)$	g kg^{-1}	5.99	6.22	6.48
$Sal^{t2}(G1)$	g kg^{-1}	6.22	6.48	6.51
Average NBL thickness	m	9.5	9.5	12.0
Salinity change due to vertical diffusion	g kg^{-1} $month^{-1}$	-0.10	-0.09	-0.08
Vertical diffusion of O_2	mmol O_2 m^{-2} h^{-1}	0.43	0.32	0.26

Formatted: English (United States)

Formatted: Outline numbered + Level: 2 + Numbering Style: 1, 2, 3, … + Start at: 1 + Alignment: Left + Aligned at: 0.63 cm + Indent at: 1.4 cm

O_2 change due to diffusion	mg l^{-1} $month^{-1}$	1.05	0.78	0.50
O_2 change due to advection	mg l^{-1} $month^{-1}$	0.48	1.24	0.68
O_2 change due to consumption	mg l^{-1} $month^{-1}$	4.20	4.24	2.94
O_2 consumption rate	**mmol O_2 m^{-2} h^{-1}**	**1.72**	**1.75**	**1.53**

For the periods when inflows through the Irbe Strait are absent, the only physical process contributing to the changes in oxygen concentration in the gulf NBL is vertical diffusion/mixing. We suggested that such conditions of no inflows occurred in summer 2015, based on prevailing winds (Fig. 8b) and observed low salinity in the NBL at station G1 (Table 1). The vertical diffusive flux of oxygen was estimated at 0.49 mmol m^{-2} h^{-1} for April-November 2015. If considering a similar oxygen consumption rate in 2015 as in 2018 (1.67 mmol O_2 m^{-2} h^{-1}), oxygen depletion in the NBL could be 1.70 mg l^{-1} $month^{-1}$, taking into account the estimated average NBL thickness of 16 m in summer 2015. Thus, this rate is enough to cause hypoxia in the near-bottom layer of the central gulf in late October 2015, as it was observed (see Figs. 2 and 3), but not earlier.

Simultaneously with the development of hypoxia, phosphate concentrations increased in the NBL at station G1 in summer 2018 (Fig. 9). The phosphate concentrations were already elevated in July when oxygen concentrations did not indicate hypoxic conditions at 2-3 m from the seabed. However, hypoxia could occur at the sediment-water interface. The changes in phosphate concentrations due to physical processes and the amount of phosphates released from the sediments were estimated using the same approach as was applied for estimating oxygen consumption (see Sect. 2). As seen in Table 3, the changes in phosphate concentrations due to advection and lateral mixing were larger than due to vertical diffusion. Considering both physical processes, the concentration estimates were lower than the measured values on the next monitoring campaign. This difference between the measured and estimated concentrations was assigned to the sediment release of phosphates. The largest estimated phosphate flux from the sediments was 13.6 µmol m^{-2} h^{-1} for the period from the end of May to mid-July 2018. From late April to late May, the phosphate flux from the sediments was minimal, which might be explained by relatively high oxygen concentrations in the NBL. Although the oxygen concentrations decreased and fell below the hypoxia threshold from mid-July to late August, the estimated sediment release was lower for this period (~~13.6~~7.4 µmol m^{-2} h^{-1}) than ~~the preceding period (~~from late May to mid-July~~).~~.

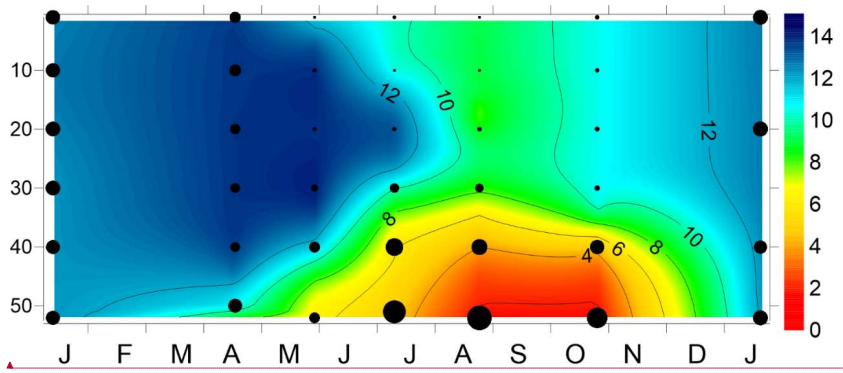

Figure ~~11~~9. Time series of vertical distribution of oxygen and phosphate concentration at station G1 in the Gulf of Riga from January 2018 to January 2019. Phosphate concentrations are indicated as black dots. The size of the dots is proportional to the measured concentrations ranging from the lower detection range of 0.06 to 2.25 µM.

Formatted: English (United States)

Table 23. Estimated changes in NBL phosphate concentration due to advection and diffusion and estimated sediment release of phosphates in the Gulf of Riga between the monitoring campaigns in 2018. Parameters measured in or estimated for monitoring campaigns' start/end are denoted by t1/t2.

Period start (t1) and end (t2)		18.04.2018-30.05	30.05.2018-11.07	11.07.2018-25.08
Period end (t2)		30.05.2018	11.07.2018	25.08.2018
$PO_4^{t1}(114)$ (µM)	µM	0.49	0.21	0.33
$PO_4^{t1}(G1)$ (µM)	µM	1.12	0.82	1.95
$PO_4^{t2m}(G1)$ (measured, µM)	µM	0.82	1.95	2.11
Average NBL thickness	m	9.5	9.5	12.0
$PO_4^{t2}(G1)$ estimatedO_4 change due to advection and lateral mixing (µM)diffusion	µM month^{-1}	-0.8404	-0.5705	1.63-0.13
$PO_4^{t2}(G1) - PO_4^{t1}(G1)O_4$ change due to advection and lateral mixing (µM)	µM month^{-1}	-0.2820	-0.2518	-0.3221
$PO_4^{t2}(G1) - PO_4^{t1}(G1)$ due to diffusion (µM)		-0.06	-0.07	-0.19
NBL thickness (m)		9.5	9.5	12.0
Estimated rate of the sediment PO_4 release (µM m^{-2} h^{-1})	**(µM m^{-2} h^{-1})**	**0.4**	**13.6**	**7.4**

Formatted ... [1]
Inserted Cells
Formatted: English (United States)
Formatted Table
Formatted: English (United States)
Formatted: English (United States)
Formatted: English (United States)
Formatted Table
Formatted ... [2]
Inserted Cells
Formatted: English (United States)
Formatted ... [3]
Formatted: English (United States)
Formatted ... [4]
Formatted: English (United States)
Formatted: Font: 9 pt, English (United States)
Formatted ... [5]
Inserted Cells
Formatted ... [6]
Formatted ... [7]
Formatted: English (United States)
Formatted: Font: 9 pt, English (United States)
Formatted Table
Formatted ... [8]
Formatted ... [9]
Formatted: English (United States)
Formatted: English (United States)
Formatted: Font: 9 pt, English (United States)
Formatted Table
Formatted: English (United States)
Inserted Cells
Formatted: English (United States)
Formatted: Left, Line spacing: single

4. ~~4~~ Discussion

~~The Gulf of Riga, a relatively shallow basin with limited water exchange with the open Baltic Sea and considerable nutrient loads from rivers, is strongly affected by eutrophication (HELCOM, 2018b). Based on data from 1963 to 1990, a statistically significant dissolved oxygen decrease in August was found for the entire 20-50 m layer in the gulf~~Declining oxygen levels and more frequent hypoxia have been reported in many coastal environments, including the Baltic Sea (Caballero-Alfonso et al., 2015; Carstensen et al., 2014; Conley et al., 2009). The present study concludes that the decreasing trend in oxygen concentrations in the Gulf of Riga near-bottom layer in summer–autumn stated earlier ~~(Berzinsh, 1995). From the late 1980s to 2006, the means of the lowest 25% of oxygen concentrations measured 1 m above the seabed in autumn ranged between 1.8 and 4.8 ml l^{-1} (2.6 and 6.9 mg l^{-1}) without an apparent trend (HELCOM, 2009). The present study points to the decreasing trend in summer–autumn oxygen concentrations since 2005 in the Gulf of Riga near-bottom layer and occasional hypoxia events. We found seven out of 14 years (2005–2018) when the near-bottom oxygen concentration during summer–autumn was <2.9 mg l^{-1}. In the years, when hypoxia occurred, seasonal stratification was typically enhanced by the vertical salinity distribution, often with higher salinity in the near-bottom layer. In 2018, fast warming of the surface layer in spring and spreading of saltier waters into the near-bottom layer in the first half of the year resulted in strong vertical stratification and extensive hypoxic area in the gulf in August–October. Thus, it seems that hypoxic conditions develop in the near-bottom layer if stratification is strengthened, hindering vertical mixing. However, the factors contributing to the occurrence and severity of near-bottom hypoxia have to be analyzed in more detail since the inflow of saltier waters, if originating from the near-surface layer,~~(Berzinsh, 1995; HELCOM, 2009) has continued since 2005. Near-bottom oxygen concentration fell below the hypoxia threshold in seven out of the analyzed 14 years (2005–2018), and the largest area of hypoxic bottoms was revealed in 2018. It is well known and documented that the main causes of near-bottom hypoxia are elevated nutrient inputs, leading to high oxygen demand for organic matter decomposition, and topographic/hydrographic characteristics of coastal areas, restricting oxygen supply by physical processes (Carstensen et al., 2014; Virtanen et al., 2019). If oxygen consumption rate exceeds oxygen supply by vertical mixing and advection for a long enough period, hypoxia or even anoxia could occur (Fennel and Testa, 2019).

Since oxygen consumption at the sediment-water interface can have a large share in depth-integrated respiration (Boynton et al., 2018), separation of the near-bottom layer from the waters above may accelerate oxygen depletion in the NBL. For instance, Jokinen et al. (2018) suggested that a decrease of the water volume between the pycnocline and the seabed increased the probability of hypoxia occurrences in a shallow basin of the Archipelago Sea (Haverö). We identified that near-bottom hypoxia in the central Gulf of Riga was often associated with higher NBL salinity that can be a result of inflows through the Irbe Strait (Lilover et al., 1998; Skudra and Lips, 2017). However, if originating from the near-surface layer, the inflows of saltier waters should feed the near-bottom layer of an enclosed basin with oxygen (e.g. Schmidt et al., 2021).

Formatted: Outline numbered + Level: 1 + Numbering Style: 1, 2, 3, … + Start at: 1 + Alignment: Left + Aligned at: 0 cm + Indent at: 0.63 cm

~~We suggest that, in addition to the enhanced water column stratification, certain other factors or processes, and the timing, how and when the vertical stratification developed, contributed to the observed extensive hypoxia in 2018. Conditions, favoring larger than usual oxygen depletion, were pre-set already by exceptionally large river runoff at the end of 2017 and the beginning of 2018 since larger river runoffs during autumn-winter raise the nutrient and organic matter concentrations in the gulf (Yurkovskis, 2004). Not fully mixed water column in the gulf deep area after the winter season 2018 could be the other important factor. In late spring, the gulf' water column is usually homogenous (Skudra and Lips, 2017; Stipa et al., 1999), but in April 2018, we observed vertical salinity and dissolved oxygen gradients in the deep layer. The appearance of the saltier near-bottom layer matches with the observed easterly winds in February-March 2018~~Based on the introduced method, the oxygen consumption rate was estimated at 1.67 mmol O_2 m^{-2} h^{-1} for spring-summer 2018, comparable with the earlier measurements and calculations. ~~which could create the inflows of Baltic Proper waters through the Irbe Strait (Lips et al., 1995; Raudsepp and Elken, 1995).~~

~~A detailed comparison of oxygen dynamics between the years 2018 and 2017 indicated that the largest difference was a drastic drop of near-bottom oxygen concentrations in April-May 2018. It could be related to the existing haline stratification in the deep layer and, thus, restricted vertical mixing, while dissolved oxygen consumption was intensified due to the settling of the vernal bloom (Olli and Heiskanen, 1999). High heat flux through the sea surface and weakest winds in May 2018 compared to all other years caused strong thermal stratification and weak vertical mixing. In 2017, such a decrease in oxygen concentrations did not occur (although we could assume a similar oxygen consumption due to the settling spring bloom) since the water column was not stratified yet, and dissolved oxygen could be transported to the near-bottom layer from the upper water layers. Furthermore, the near-bottom mixed (weakly stratified) layer extended from the seabed to the depths of 38.5 m to 30.5 m in May-August 2017, while its thickness did not exceed 12 m in 2018 (from the seabed to 42 m depth). It could be a reason for more pronounced oxygen depletion in 2018 than in 2017. This effect of stronger depletion in 2018 is similar to the suggestion by Jokinen et al. (2018) that a decrease of the water volume between the pycnocline and the seabed increases the probability of hypoxia occurrences.~~

~~From mid-July to the end of August 2018, salinity in the near-bottom layer did not increase considerably anymore, but oxygen concentrations dropped below the hypoxia threshold. Thus, almost no saltier water inflows into the near-bottom layer existed in late summer 2018, and lateral advection and mixing could not supply additional oxygen there. It agrees with the prevailing downwelling-favorable winds along the EGB coast near the Irbe Strait since the beginning of August, which did not support the inflows anymore. The observed changes in the upper mixed layer depth also could contribute to the lack of inflows. As seen from the buoy profiler data, strong winds caused a deepening of the upper mixed layer in mid-August 2018. Such sharp or gradual deepening of the upper mixed layer, expected during summer months (from June to August) in the Gulf of Riga and similar basins (Liblik and Lips, 2011; Stipa et al., 1999), also influences the characteristics of the inflow water. If even the~~

inflows occur, the waters could be too warm (since originating from the warm upper layer or thermocline), and as described by Liblik et al. (2017), such inflows could occur as buoyant sub-surface intrusions. As a result, the near-bottom layer of the gulf would not receive additional oxygen through lateral transport. We conclude that since mid-August, due to both missing inflow favorable winds and deepening of the thermocline, lateral transport to the deepest part of the gulf was almost absent, and hypoxia developed there.

A way to describe the level of eutrophication is to estimate the amount of oxygen consumed by organic material degradation (Carstensen et al., 2014; Stoicescu et al., 2019). Because the inflowing saltier Baltic Proper waters have higher oxygen concentration than oxygen concentrations in the central Gulf of Riga near-bottom layer, hypoxia has to be locally developed. We estimated oxygen consumption rates for the central gulf using an indirect method by assuming that the changes in the near-bottom oxygen concentrations were mostly driven by advection and lateral mixing (inflow of saltier waters through the Irbe Strait), vertical diffusion and local consumption. Vertical mixing is incorporated in the introduced method considering a complete mixing in the limits of the NBL and diffusive flux between the NBL and upper layers defined by the vertical gradient and turbulent diffusion coefficient depending on the strength of the vertical stratification (e.g., Stoicescu et al. (2019)). Note that this method of estimating diffusion is applicable only in the case of stable stratification and vertical gradients, not varying too much. For instance, in the case of complete mixing of the water column, it could not be applied. We got an average consumption rate estimate of 1.67 mmol O_2 m^{-2} h^{-1} from mid-April to late August 2018.

The reliability of the introduced method is also related to the chosen time step and the use of single profiles acquired once a month or more seldom. If considering an average water speed of 5 cm s^{-1} (e.g. Lips et al., 2016; Soosaar et al., 2014) and the distance from the Irbe Strait to the Ruhnu Deep of 120 km, the 'traveling' duration of an inflowing water mass would be about 28 days. Thus, the monitoring campaigns apart 1-1.5 months could be acceptable for applying this method since the time step between the measurements is long enough. To assess the potential error of using infrequent profiles (although sampled at almost regular dates), we found consumption rates based on high-frequency profiler data with up to 8 profiles a day for about two weeks on 5-21 August 2018 (Fig. 12). Monitoring profiles from late May 2018 were selected as the starting point for the estimations. Based on profiler data, we found the mean consumption rate value of 1.53 mmol O_2 m^{-2} h^{-1}. The standard deviation of the estimates was 0.37 mmol O_2 m^{-2} h^{-1} and coefficient of variation 25 %.

On the one hand, it was a surprise that the results were relatively stable since, as shown above, the variability in the near-bottom layer was quite high on 5-21 August 2018. On the other hand, it was expected since this variability could mostly be assigned to the advection and changes in the thickness of the near-bottom layer at the measurement site, but not to the mixing with the water column above the NBL. The mean consumption rate estimated using buoy profiler data (1.53 mmol O_2 m^{-2} h^{-1}) is almost the same as the average for 2018 based on monitoring campaigns from late May to late August (1.64 mmol O_2 m^{-2} h^{-1}). We conclude that the method can be used even based on scarce monitoring profiles, but one must remember the

~~uncertainties. In our case, the standard error was 0.37 mmol O_2 m^{-2} h^{-1} and relatively large variability of the estimates even between the profiles collected during the same day can be noticed (Fig. 12). In extreme cases, the estimates could differ up to 2 times (from <1 to >2 mmol O_2 m^{-2} h^{-1}) that makes using single profiles rather unreliable and should encourage to increase the monitoring frequency and the use of profilers (Mack et al., 2020).~~

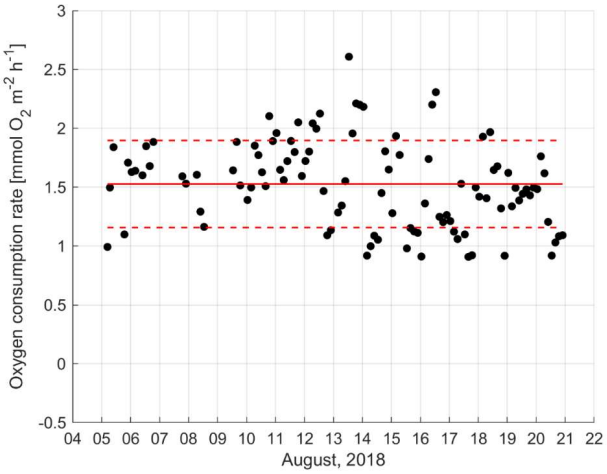

~~Figure 12. Oxygen consumption rates estimated using buoy profiler data from 3-18 August 2018 and monitoring data on 30 May 2018 as the salinity and dissolved oxygen values of the "old" waters (station G1) and inflowing waters (station 114). Red solid line represents the mean oxygen consumption rate of 1.53 mmol O_2 m^{-2} h^{-1}. Red dashed lines represent the standard deviation bounds.~~

~~Our average consumption rate estimates for the spring-summer of 2018 – based on monitoring campaigns from late April to late August (1.67 mmol O_2 m^{-2} h^{-1}) and monitoring and profiler data from late May to August (1.53 mmol O_2 m^{-2} h^{-1}) – are comparable with the earlier measurements and calculations.~~ Results from this study are higher than the estimates of consumption rates obtained for the Baltic Proper and the Gulf of Finland – 0.11-0.39 mmol O_2 m^{-2} h^{-1} (Koop et al., 1990) and 0.46-0.53 mmol O_2 m^{-2} h^{-1} (Conley et al., 1997), respectively, and closer to but slightly lower than the estimates based on the direct measurements in the Gulf of Riga by Aigars et al. (2015) – on average 2.3 mmol O_2 m^{-2} h^{-1}. One reason ~~of~~for the lower values obtained in our study might be related to the fact that the analysis by Aigars et al. (2015) was conducted using core samples collected at stations 119 and 120, which are situated in the southern Gulf of Riga ~~close to the main river mouths (see~~

Formatted: English (United States)

Fig. 1)., close to the main river mouths (see Fig. 1). On the other hand, our estimates are much higher than found for the deep areas of the Baltic Proper, although it is stated that the consumption rates there are recently accelerated (Meier et al., 2018).

Possible future changes in climate, including warming that causes the strengthening of stratification and decreased oxygen solubility, and changes in precipitation/river runoff, influence the extent of hypoxia in the Baltic Sea (Meier et al., 2011). Jokinen et al. (2018) have suggested that in addition to the changes in anthropogenic nutrient loads and climate change, the long-term alteration in morphology, leading to increased source-to-sink ratio and the decrease of the bottom water volume, could increase the vulnerability to hypoxia in enclosed basins (separated from the open sea areas by sills). We add that basin-specific relationships between the basin morphology (e.g., sill depth) and stratification parameters (e.g., UML depth) should be considered. If the sill depth is less than the thermocline depth, the inflows could not reach the near-bottom layer in the deeper parts of the enclosed basins like the inflows into the Gulf of Riga via the Suur Strait. If the depths of the thermocline and the sill in the connecting strait are comparable, then due to an average deepening of the thermocline during the summer months (Liblik and Lips, 2011), such conditions of no inflows into the NBL of deeper areas occur more often in late summer-autumn. In the very long run, the shoaling of the sills in the northern Baltic Sea due to glacio-isostatic uplift (with a rate of up to 4 mm y^{-1}; e.g., Mäkinen and Saaranen, 1998) could be a reason for more frequent hypoxia today than hundreds years ago.

Strong vertical stratification has been considered as a major factor restricting oxygen supply to the NBL due to its strength (Kralj et al., 2019) and duration (Fennel and Testa, 2019). Stratification has strengthened in the Baltic Sea mostly due to the increase in surface layer temperature (Kniebusch et al., 2019; Liblik and Lips, 2019). In our assessment of the development of vertical stratification according to Simpson et al. (1990), the surface heat flux and wind-induced mixing were the main contributors. River runoff had in general lower contribution to the development of stratification although haline stratification is often observed in Baltic Sea basins in winter-early spring (Liblik et al., 2020a; Stipa et al., 1999), as also revealed in the Gulf of Riga for the year with the highest river discharge – 2013. In addition, large river runoff could raise the nutrient and organic matter concentrations in the gulf (Yurkovskis, 2004) and, hence, contribute to the hypoxia development.

In 2018, fast warming of the surface layer and weak wind-induced mixing in spring resulted in strong vertical stratification. The peak of the spring bloom, which generates most of the sedimented organic material, is observed in the Gulf of Riga in April-May (Olli and Heiskanen, 1999; Purina et al., 2018). When the spring bloom material reaches the sediment surface, it triggers enhanced oxygen consumption., with the rate and delay depending on the bloom species composition, e.g., diatom-dinoflagellate ratio (Spilling et al., 2018). Aigars et al. (2015) found higher consumption rates in late spring-early summer than in late summer-autumn and related this result to the availability of organic material, i.e., settling of spring bloom. Our results with high consumption rates from May to mid-July 2018 agree with their estimates and interpretation. Thus, the strength of stratification in spring, including its early development, summer is a crucial factor influencing the extent of seasonal hypoxia in the Gulf of Riga and similar coastal basins. In general, a longer duration of the stratified season, including earlier onset of

Formatted: English (United States)

Formatted: English (United States)

Formatted: English (United States)

the years with weak or absent stratification (as 2017), such a decrease in oxygen concentrations did not occur (although we could assume a similar oxygen consumption due to the settling spring ~~and later decay of~~bloom) since dissolved oxygen could be transported to the near-bottom layer from the upper water layers.

Formatted: Font color: Auto

Formatted: Font color: Auto

Formatted: Font color: Auto

Although strong stratification is a major factor in hypoxia development, we suggest that the oxygen consumption rate in the NBL of the Gulf of Riga is high enough to lead to hypoxia even if stratification at its peak is not very strong. 2015 is an example year with relatively weak stratification and detected hypoxia – the stratified period was long enough for hypoxia to develop in late October but not earlier. The opposite situation was depicted in 2016 – vertical stratification ~~in~~ was among the strongest but hypoxia was not detected since the water column was fully mixed before the autumn~~, will lead to a more extended vegetation period~~ monitoring cruise in late October. We suggest that a longer duration of the stratified season in recent years, as also revealed by other authors, e.g., ~~(Wasmund et al., 2019) and hypoxia presence in the near-bottom layer of seasonally stratified basins.~~Wasmund et al. (2019), has increased the probability of hypoxia occurrences in the near-bottom layer of seasonally stratified coastal basins in autumn. The latter could have caused the observed sharp decline in near-bottom oxygen concentrations in the Gulf of Riga in autumn (but not in summer) during the last 15 years.

Formatted: Font color: Auto

Formatted: Font color: Auto

In April 2018, we observed vertical salinity and dissolved oxygen gradients in the deep layer. The appearance of the saltier near-bottom layer matches with the observed easterly winds in February-March 2018, which could create the inflows of Baltic Proper waters through the Irbe Strait (Lips et al., 1995; Raudsepp and Elken, 1995). A similar thin near-bottom layer with higher salinity was observed in spring 2014, and in both years, the oxygen depletion was the deepest in summer compared to the other years. The year 2018 was specific since additional inflows of saltier waters in early summer caused an uplift of the already low oxygen near-bottom waters. As a consequence, the border of hypoxic waters was at its shallowest depth, and the estimated extent of hypoxic bottoms was the largest. No further inflows in summer 2014 resulted in the lowest oxygen concentration in the NBL in 2014, and further inflows in September 2013 led to NBL oxygenation and no hypoxia in October 2013.

To answer the formulated questions, we can state that, in general, the year 2018 was in agreement with the long-term changes in the GoR oxygen dynamics – near-bottom hypoxia is developed more frequently in recent years than earlier. On the other hand, the largest extent of hypoxia was a result of the rapid warming of the surface layer and strengthening of thermal stratification and a specific sequence of inflows in spring-early summer (creating deep pycnocline) and the absence of inflows since August. Additionally, high freshwater inputs in autumn-winter 2017-2018 could bring more organic matter into the system. We further analyzed how the climate change projections could influence these factors and thus the occurrence of hypoxia in the GoR.

Earlier modelling studies have stated that possible future changes in climate, including warming that causes the strengthening of stratification and decreased oxygen solubility, and changes in precipitation/river runoff, influence the extent of hypoxia in the Baltic Sea (Meier et al., 2011). Strengthening of vertical stratification is predicted by the projected future increase in sea surface temperatures (Gröger et al., 2019; Meier and Saraiva, 2020; Saraiva et al., 2019b). Also, an increase in the total runoff to the Baltic Sea is predicted (Saraiva et al., 2019a, 2019b) that could lead to a decrease in surface salinity, but these predictions are uncertain. Although climate projections for wind are uncertain in the Baltic Sea area (Christensen et al., 2015), a slight decrease in wind speed in spring is expected (Ruosteenoja et al., 2019). Low wind speed leads to low mixing and strong stratification. Thus, in general, the future projections seem to be in favor of a strengthened stratification regime. Furthermore, weaker winds in spring create more favorable conditions for a steady outflow in the surface layer and inflow in the sub-surface layer through the Irbe Strait. When also considering a predicted winter river runoff increase due to intermittent melting (Stonevičius et al., 2017) – which would potentially bring additional nutrients to the sea – hypoxic events in the future would probably occur more often and perhaps be even more severe.

Although phosphorus inputs into the Gulf of Riga have decreased ~~(HELCOM, 2018c)~~(HELCOM, 2018b), they are still higher than maximum allowable inputs by about 1000 t year^{-1} (HELCOM, 2019). Our analysis of the long-term nutrient data revealed a statistically significant increasing trend in near-bottom phosphate and total phosphorus concentrations in the stratified season. ~~Earlier studies (e.g., Yurkovskis, 2004) and assessments (HELCOM, 2018a, 2018d) have revealed that the trends in both total phosphorus and~~ A positive correlation between the near-bottom phosphate ~~concentrations in the surface layer (as used for the referred HELCOM indicators) are unclear since the 1990s. The increase in near-bottom phosphate concentrations could be attributed to the changes in~~and oxygen concentrations points to the internal load – the release of phosphates from the bottom sediments under low oxygen concentrations (e.g. Pitkänen et al., 2001). ~~The resuspension-induced flux (e.g. Almroth et al., 2009) could have a notable contribution in the Gulf of Riga, as short-term high values of vertical shear of horizontal velocity forced by local strong wind events have been reported by Raudsepp and Kõuts (2001) in the Ruhnu Deep. However, the analyzed long-term data support the suggestion on the increased release of phosphates in conditions of more extended hypoxia in recent years – the inter-annual variability in phosphate and oxygen concentrations in summer-autumn are well correlated. We observed an increase in phosphate concentrations in the near-bottom layer~~ Using an indirect method suggested in this study, the estimated phosphate fluxes reached up to13.5 µmol m^{-2} h^{-1} from the end of May to mid-July 2018. The observed increase in phosphate concentrations in the NBL in summer 2018 already before hypoxia development~~. It~~ agrees with the results ~~obtained~~ by Aigars et al. (2015), showing that the phosphate flux did increase substantially ~~when the near-bottom~~at oxygen ~~concentrations fell below~~ concentration ≤6 mg l^{-1}.

~~We estimated phosphate fluxes using an indirect method with an assumption that the near-bottom phosphate concentrations change due to the internal load, advection and lateral mixing of inflowing waters with the gulf near-bottom waters and vertical diffusion. The fluxes estimated with a time step of approximately 1.5 months reached up to 13.5 µmol m^{-2} h^{-1} (end of May to~~

~~mid-July 2018).~~ Earlier studies by Eglīte et al. (2014) and Aigars et al. (2015) ~~have obtained similar results. They measured the changes in nutrient concentrations during 48-hour cycles of laboratory incubation of sediments under controlled oxygen concentrations varying from 1 to 10 mg l^{-1} (Eglīte et al., 2014) or corresponding to the near-bottom oxygen concentrations at the sampling site and time (Aigars et al., 2015).~~ have obtained similar estimates of the sediment phosphorus release. The average phosphate fluxes directed out of the sediments obtained by Eglīte et al. (2014) varied between 4.8 µmol m^{-2} h^{-1} at low oxygen concentrations (1-2 mg l^{-1}) and 1.8 µmol m^{-2} h^{-1} at 10 mg l^{-1}. Aigars et al. (2015) found that the average phosphate fluxes from sediments gradually increased from low values ~~(~~2-5 µmol m^{-2} h^{-1}~~)~~ in April-May to ~~10 µmol m^{-2} h^{-1} in June-July, 18 µmol m^{-2} h^{-1} in August and~~ 55 µmol m^{-2} h^{-1} in October 2012. ~~They suggested that inorganic fractions of phosphorus (and nitrogen) mineralized from organic material are retained in sediments until near-bottom water oxygen concentration is substantially decreased.~~ Our maximum flux estimates from late May to mid-July are close to the values obtained by Aigars et al. (2015) in June-August, but we did not observe a further increase of NBL phosphate concentrations in late summer-autumn ~~and the flux estimates from mid-July to late August were lower than for the preceding period~~. The sediment flux of phosphates obtained in this study also agrees with an average estimate for the coastal Gulf of Finland – 13 kg km^{-2} d^{-1} or 17 µmol m^{-2} h^{-1} (Pitkänen et al., 2001).

Formatted: English (United States)

~~5 Conclusions~~

~~We~~

We showed that the meteorological and hydrological conditions highly influence hypoxia development, and the internal load of phosphorus is linked to near-bottom oxygen conditions. This result agrees with other studies based on long-term monitoring and targeted research data stating that the phosphorus dynamics in the Gulf of Finland is also largely defined by the meteorological and hydrographic conditions (Lehtoranta et al., 2017; Lips et al., 2017). In the Baltic Sea scale, such internal load of phosphorus also supports cyanobacterial nitrogen fixation and, thus, counteracts not only external phosphorus load reduction but also external nitrogen load reduction (Savchuk, 2018).

In conclusion, we suggest that the sequence of certain processes triggered the observed extensive hypoxia in the Gulf of Riga in 2018. ~~First, haline stratification was formed in the deep layer of the central gulf in early spring, most probably due to inflows of saltier waters forced by the prevailing easterly winds in February-March 2018.~~ Enhanced seasonal stratification was created by the rapid warming of the surface layer and calm wind conditions in spring ~~leading to restricted vertical mixing. Thus, oxygen depletion due to consumption at the sediment surface was confined in the relatively thin near-bottom mixed layer already in spring when usually the water column is weakly stratified and oxygen could be supplied to the deep areas by vertical mixing. North-easterly winds that occasionally dominated in spring-summer 2018 supported the inflows of saltier waters through the Irbe Strait that maintained haline stratification in the deep layer of the gulf. In August-October, no further inflows reached the near-bottom layer of the central gulf due to unfavorable wind conditions and deepening of the thermocline, resulting in a drop of oxygen concentrations below the hypoxia threshold. Assuming that oxygen depletion in the near-bottom layer was governed by consumption at the sediment surface and lateral mixing of NBL waters and inflowing waters, and taking into account the diffusive flux between the NBL and water column above in stratified conditions, the average oxygen consumption rates in summer (in stratified conditions) was about 1.7 mmol O_2 m^{-2} h^{-1}. Thus, the substantial oxygen depletion in late summer-early autumn 2018 in the near-bottom layer, separated from the rest of the water column by a vertical salinity gradient, was created early and existed during the whole summer-autumn. The observed increase in phosphate concentrations in the hypoxic near-bottom layer in summer 2018 suggests a significant sediment phosphorus release up to 13.5 µmol m^{-2} h^{-1}. Intensification of eutrophication effects, including the observed deepening of hypoxia and increased near-bottom phosphate concentrations, could be partly associated with prolonged stratified seasons in the recent decade. We conclude, if similar meteorological conditions as in 2018 could occur more frequently, such extensive hypoxia would be more common in the future in the Gulf of Riga and other coastal basins with similar morphology and human-induced elevated input of nutrients.~~, leading to restricted vertical mixing. In spring-early summer, inflows of saltier waters through the Irbe Strait maintained haline stratification, keeping the near-bottom layer relatively thin and further restricting the vertical mixing. However, we showed that the estimated average oxygen consumption rate is large enough to lead to near-bottom hypoxia in conditions of weaker stratification but a prolonged stratified season. The projections of meteorological and hydrological conditions anticipate that

the frequency and extent of hypoxia will likely increase in the future. Since the internal load of phosphorus is linked to the near-bottom oxygen conditions, this scenario also predicts no fast reduction of nutrient concentrations in the Gulf of Riga and similar coastal basins.

Data availability

Historical and forcing data can be found in databases (see Sect.2). CTD data are available via SeaDataNet. Buoy profiler data are available upon request.

Author contribution

S-TS was the main responsible person for developing methods, analyzing data, and writing the manuscript. UL and JL contributed to developing methods and writing the manuscript. TL contributed by analyzing the data and reviewing the manuscript. MS provided river inflow and Latvian CTD data and contributed to reviewing the manuscript. OS contributed by collecting and analyzing CTD data. IL contributed by analyzing the nutrient data and reviewing the manuscript.

Competing interests

The authors declare that they have no conflict of interest.

Acknowledgements

We thank the agencies and institutes funding and implementing the marine environmental monitoring programs in Estonia and Latvia. Data were provided through the Estonian environmental monitoring information system (KESE), Latvian environmental monitoring database (Latvian Environmental, Geology and Meteorology Center), HELCOM/ICES database, SeaDataNet Pan-European infrastructure for ocean and marine data management, and Copernicus Climate Change Service information. We are thankful to the crew of RV Salme and colleagues who participated in the cruises, and data exploration (Ilja Maljutenko for the help with ERA5 data). This work was supported by the Estonian Ministry of Education institutional research funding (IUT19-6), the Estonian Research Council grant (PRG602) and the joint Baltic Sea research and development program (Art 185) through Grant 03F0773A (BONUS INTEGRAL).

References

Aigars, J. and Carman, R.: Seasonal and spatial variations of carbon and nitrogen distribution in the surface sediments of the Gulf of Riga, Baltic Sea, Chemosphere, 43, 313–320, 2001.

Aigars, J., Poikāne, R., Dalsgaard, T., Eglīte, E. and Jansons, M.: Biogeochemistry of N, P and SI in the Gulf of Riga surface sediments: Implications of seasonally changing factors, Cont. Shelf Res., 105, 112–120, 2015.

~~Almroth, E., Tengberg, A., Andersson, J. H., Pakhomova, S. and Hall, P. O. J.: Effects of resuspension on benthic fluxes of oxygen, nutrients, dissolved inorganic carbon, iron and manganese in the Gulf of Finland, Baltic Sea, Cont. Shelf Res., 29(5), 807–818, doi:https://doi.org/10.1016/j.csr.2008.12.011, 2009.~~

~~Ammerman, J.: QuikChem® Method 31-115-01-1-I Determination of Orthophosphate by Flow Injection Analysis, Lachat Instruments, 2001.~~

Astok, V., Otsmann, M. and Suursaar, Ü.: Water exchange as the main physical process in semi-enclosed marine systems: the Gulf of Riga case, Hydrobiologia, 393 [online] Available from: https://link.springer.com/content/pdf/10.1023/A:1003517110726.pdf, 1999.

Berzinsh, V.: Hydrology, in Ecosystem of the Gulf of Riga between 1920-1990, edited by E. Ojaveer, pp. 7–31, Estonian Academy Publishers, Tallinn., 1995.

Bindoff, N. L., Cheung, W. W. L., Kairo, J. G., Arístegui, J., Guinder, V. A., Hallberg, R., Hilmi, N., Jiao, N., Karim, M. S., Levin, L., O'Donoghue, S., Cuicapusa, S. R. P., Rinkevich, B., Suga, T., Tagliabue, A. and Williamson, P.: Changing Ocean, Marine Ecosystems, and Dependent Communities., in IPCC Special Report on the Ocean and Cryosphere in a Changing Climate, edited by H.-O. Pörtner, D. C. Roberts, V. Masson-Delmotte, P. Zhai, M. Tignor, E. Poloczanska, K. Mintenbeck, A. Alegría, M. Nicolai, A. Okem, J. Petzold, B. Rama, and N. M. Weyer, In press., 2019.

Bonsdorff, E., Diaz, R. J., Rosenberg, R., Norkko, A. and Cutter Jr, G. R.: Characterization of soft-bottom benthic habitats of the Åland Islands, norther Baltic Sea, Mar. Ecol. Prog. Ser., 142, 235–245, 1996.

Boynton, W. R., Ceballos, M. A. C., Bailey, E. M., Hodgkins, C. L. S., Humphrey, J. L. and Testa, J. M.: Oxygen and Nutrient Exchanges at the Sediment-Water Interface: a Global Synthesis and Critique of Estuarine and Coastal Data, Estuaries and Coasts, 41(2), 301–333, doi:10.1007/s12237-017-0275-5, 2018.

Caballero-Alfonso, A. M., Carstensen, J. and Conley, D. J.: Biogeochemical and environmental drivers of coastal hypoxia, J. Mar. Syst., 141, 190–199, 2015.

Carstensen, J., Andersen, J. H., Gustafsson, B. G. and Conley, D. J.: Deoxygenation of the Baltic Sea during the last century, Proc. Natl. Acad. Sci. U. S. A., 111(15), 5628–33 [online] Available from: http://www.pubmedcentral.nih.gov/articlerender.fcgi?artid=3992700&tool=pmcentrez&rendertype=abstract, 2014.

Christensen, O. B., Kjellström, E. and Zorita, E.: in Second Assessment of Climate Change for the Baltic Sea Basin, in Second Assessment of Climate Change for the Baltic Sea Basin, edited by BACC II Author Team, pp. 217–233, Springer International Publishing., 2015.

Codiga, D. L., Stoffel, H. E., Decautis, C. F., Kiernan, S. and Oviatt, C. A.: Narragansett Bay Hypoxic Event Characteristics Based on Fixed-Site Monitoring Network Time Series: Intermittency, Geographic Distribution, Spatial Synchronicity, and Interannual Variability, Estuaries and Coasts, 32, 621–641, doi:10.1007/s12237-009-9165-9, 2009.

Conley, D. J., Stockenberg, A., Carman, R., Johnstone, R. W., Rahm, L. and Wulff, F.: Sediment-water Nutrient Fluxes in the Gulf of Finland, Baltic Sea, Estuar. Coast. Shelf Sci., 45(5), 591–598, 1997.

Conley, D. J., Humborg, C., Rahm, L., Savchuk, O. P. and Wulff, F.: Hypoxia in the Baltic Sea and Basin-Scale Changes in Phosphorus Biogeochemistry, Envrion. Sci. Technol., 36, 5315–5320 [online] Available from: http://pubs.acs.org/doi/pdf/10.1021/es025763w, 2002.

Conley, D. J., Carstensen, J., Ærtebjerg, G., Christensen, P. B., Dalsgaard, T., Hansen, J. L. S. and Josefson, A. B.: LONG-TERM CHANGES AND IMPACTS OF HYPOXIA IN DANISH COASTAL WATERS, Ecol. Appl., 17(sp5), S165–S184, doi:https://doi.org/10.1890/05-0766.1, 2007.

Conley, D. J., Björck, S., Bonsdorff, E., Carstensen, J., Destouni, G., Gustafsson, B. G., Hietanen, S., Kortekaas, M., Kuosa, H., Meier, H. E. M., Müller-Karulis, B., Nordberg, K., Norkko, A., Nürnberg, G., Pitkänen, H., Rabalais, N. N., Rosenberg, R., Savchuk, O. P., Slomp, C. P., Voss, M., Wulff, F. and Zillén, L.: Hypoxia-Related Processes in the Baltic Sea, Environ. Sci. Technol., 43(10), 3412–3420 [online] Available from: http://pubs.acs.org/doi/abs/10.1021/es802762a, 2009.

Conley, D. J., Carstensen, J., Aigars, J., Axe, P., Bonsdorff, E., Eremina, T., Haahti, B.-M., Humborg, C., Jonsson, P., Kotta, J., Lännegren, C., Larsson, U., Maximov, A., Medina, M. R., Lysiak-Pastuszak, E., Remeikaitė-Nikienė, N., Walve, J., Wilhelms, S. and Zillén, L.: Hypoxia Is Increasing in the Coastal Zone of the Baltic Sea, Environ. Sci. Technol., 45(16), 6777–6783, doi:10.1021/es201212r, 2011.

~~Egan, L.: QuikChem® Method 31-107-04-1-D Determination of Nitrate and/or Nitrite in Brackish Waters by Flow Injection Analysis., Lachat Instruments, 2000.~~

Diaz, R. J. and Rosenberg, R.: Spreading Dead Zones and Consequences for Marine Ecosystems, Science (80-.)., 321(5891), 926–929, doi:10.1126/science.1156401, 2008.

Eglīte, E., Lavrinovičs, A., Müller-Karulis, B., Aigars, J. and Poikāne, R.: Nutrient turnover at the hypoxic boundary: flux measurements and model representation for the bottom water environment of the Gulf of Riga, Baltic Sea, Oceanologia, 56(4), 711–735, 2014.

EMODnet Bathymetry Consortium: EMODnet Digital Bathymetry (DTM), , doi:https://doi.org/10.12770/bb6a87dd-e579-4036-abe1-e649cea9881a, 2020.

Fennel, K. and Testa, J. M.: Biogeochemical Controls on Coastal Hypoxia, Ann. Rev. Mar. Sci., 11(1), 105–130, doi:10.1146/annurev-marine-010318-095138, 2019.

Groeskamp, S. and Iudicone, D.: The Effect of Air-Sea Flux Products, Shortwave Radiation Depth Penetration, and Albedo on the Upper Ocean Overturning Circulation, Geophys. Res. Lett., 45(17), 9087–9097, doi:https://doi.org/10.1029/2018GL078442, 2018.

Gröger, M., Arneborg, L., Dieterich, C., Höglund, A. and Meier, H. E. M.: Summer hydrographic changes in the Baltic Sea,

Kattegat and Skagerrak projected in an ensemble of climate scenarios downscaled with a coupled regional ocean–sea ice–atmosphere model, Clim. Dyn., 53(9), 5945–5966, doi:10.1007/s00382-019-04908-9, 2019.

Gustafsson, B. G., Schenk, F., Blenckner, T., Eilola, K., Meier, H. E. M., Müller-Karulis, B., Neumann, T., Ruoho-Airola, T., Savchuk, O. P. and Zorita, E.: Reconstructing the Development of Baltic Sea Eutrophication 1850–2006, Ambio, 41, 534–548, 2012.

Hansson, M. and Viktorsson, L.: REPORT OCEANOGRAPHY No. 70, 2020. Oxygen Survey in the Baltic Sea 2020 - Extent of Anoxia and Hypoxia, 1960-2020., 2020.

HELCOM: Environment of the Baltic Sea area 1994-1998, Balt. Sea Environ. Proc. No. 82B, 215, 2002.

HELCOM: Eutrophication in the Baltic Sea - An Integrated thematic assessment of the effects of nutrient enrichment and eutrophication in the Baltic Sea region, Balt. Sea Environ. Proc. No. 115B, 148, 2009.

HELCOM: STATE OF THE BALTIC SEA 2017 - HELCOM Second Holistic Assessment of the Ecosystem Health Of the Baltic Sea (HOLAS II), [online] Available from: http://www.helcom.fi/helcom-at-work/projects/holas-ii, 2016.

HELCOM: ~~Dissolved inorganic phosphorus (DIP). ~~Manual for the Marine Monitoring in the COMBINE Programme of HELCOM~~ core indicator report. Online.,~~ [online] Available from: https://helcom.fi/~~wp-content/uploads/2019/08/Dissolved-inorganic-phosphorus-DIP-HELCOM-core-indicator-2018.pdf (Accessed 31 March 2021a), 2018~~action-areas/monitoring-and-assessment/monitoring-guidelines/combine-manual/, 2017.

HELCOM: HELCOM thematic assessment of eutrophication 2011-2016., ~~2018b~~2018a.

HELCOM: Sources and pathways of nutrients to the Baltic Sea., Balt. Sea Environ. Proc. 153, ~~2018c.~~

~~HELCOM: Total phosphorus. HELCOM core indicator report. Online., 2018d~~2018b.

HELCOM: Inputs of nutrients to the sub-basins. HELCOM core indicator report. Online., 2019.

Hersbach, H., Bell, B., Berrisford, P., Biavati, G., Horányi, A., Muñoz Sabater, J., Nicolas, J., Peubey, C., Radu, R., Rozum, I., Schepers, D., Simmons, A., Soci, C., Dee, D. and Thépaut, J.-N.: ERA5 hourly data on single levels from 1979 to present., Copernicus Clim. Chang. Serv. Clim. Data Store, doi:10.24381/cds.adbb2d47, 2018.

Hoy, A., Hänsel, S. and Maugeri, M.: An endless summer: 2018 heat episodes in Europe in the context of secular temperature variability and change, Int. J. Climatol., 40, 6315–6336, doi:10.1002/joc.6582, 2020.

IOC, SCOR and IAPSO: The International Thermodynamic Equation of Seawater - 2010: Calculation and Use of Thermodynamic Properties, Intergovernmental Oceanographic Commission, Manuals and Guides No. 56. UNESCO (English), , 196, 2010.

Jansson, A., Klais-Peets, R., Grinienė, E., Rubene, G., Semenova, A., Lewandowska, A. and Engström-Öst, J.: Functional shifts in estuarine zooplankton in response to climate variability, Ecol. Evol., 10(20), 11591–11606, doi:https://doi.org/10.1002/ece3.6793, 2020.

Johansson, J.: Total and regional runoff to the Baltic Sea, HELCOM Balt. Sea Environ. Fact Sheets. Online, 2016.

Jokinen, S. A., Virtasalo, J. J., Jilbert, T., Kaiser, J., Dellwig, O., Arz, H. W., Hänninen, J., Arppe, L., Collander, M. and Saarinen, T.: A 1500-year multiproxy record of coastal hypoxia from the northern Baltic Sea indicates unprecedented

deoxygenation over the 20th century, Biogeosciences, 15, 3975–4001, 2018.

Kabel, K., Moros, M., Porsche, C., Neumann, T., Adolphi, F., Andersen, T. J., Siegel, H., Gerth, M., Leipe, T., Jansen, E. and Damsté, J. S. S.: Impact of climate change on the Baltic Sea ecosystem over the past 1,000 years, Nat. Clim. Chang., 2, 871–874, 2012.

Karlson, K., Rosenberg, R. and Bonsdorff, E.: Temporal and spatial large-scale effects of eutrophication and oxygen deficiency on benthic fauna in Scandinavian and Baltic waters-a review, Oceanogr. Mar. Biol. an Annu. Rev., 40, 427–489, 2002.

Kniebusch, M., Meier, H. E. M., Neumann, T. and Börgel, F.: Temperature Variability of the Baltic Sea Since 1850 and Attribution to Atmospheric Forcing Variables, J. Geophys. Res. Ocean., 124(6), 4168–4187, doi:https://doi.org/10.1029/2018JC013948, 2019.

Koop, K., Boynton, W. R., Wulff, F. and Carman, R.: Sediment-water oxygen and nutrient exchanges along a depth gradient in the Baltic Sea, Mar. Ecol. Prog. Ser., 63, 65–77, 1990.

~~Liblik, T. and Lips, U.: Characteristics and variability of the vertical thermohaline structure in the Gulf of Finland in summer, Boreal.Environ.Res, 16A, 73–83, 2011.~~

Kralj, M., Lipizer, M., Čermelj, B., Celio, M., Fabbro, C., Brunetti, F., Francé, J., Mozetič, P. and Giani, M.: Hypoxia and dissolved oxygen trends in the northeastern Adriatic Sea (Gulf of Trieste), Deep Sea Res. Part II Top. Stud. Oceanogr., 164, 74–88, doi:https://doi.org/10.1016/j.dsr2.2019.06.002, 2019.

Lehtoranta, J., Savchuk, O. P., Elken, J., Kim, D., Kuosa, H., Raateoja, M., Kauppila, P., Räike, A. and Pitkänen, H.: Atmospheric forcing controlling inter-annual nutrient dynamics in the open Gulf of Finland, J. Mar. Syst., 171, 4–20, 2017.

Liblik, T. and Lips, U.: Variability of synoptic-scale quasi-stationary thermohaline stratification patterns in the Gulf of Finland in summer 2009, Ocean Sci., 8(4), 603–614, doi:https://doi.org/10.5194/os-8-603-2012, 2012.

Liblik, T~~., Laanemets, J., Raudsepp, U., Elken, J. and Suhhova, I.: Estuarine circulation reversals and related rapid changes in winter near-bottom oxygen conditions in the Gulf of Finland, Baltic Sea, Ocean Sci., 9, 917–930, 2013~~. and Lips, U.: Stratification Has Strengthened in the Baltic Sea – An Analysis of 35 Years of Observational Data, Front.Earth.Sci., 7:174, doi:10.3389/feart.2019.00174, 2019.

Liblik, T., Skudra, M. and Lips, U.: On the buoyant sub-surface salinity maxima in the Gulf of Riga, Oceanologia, 59, 113–128, 2017.

Liblik, T., Väli, G., Lips, I., Lilover, M.-J., Kikas, V. and Laanemets, J.: The winter stratification phenomenon and its consequences in the Gulf of Finland, Baltic Sea, Ocean Sci., 16, 1475–1490 [online] Available from: https://doi.org/10.5194/os-16-1475-2020, 2020a.

Liblik, T., Wu, Y., Fan, D. and Shang, D.: Wind-driven stratification patterns and dissolved oxygen depletion off the Changjiang (Yangtze) Estuary, Biogeosciences, 17, 2875–2895, doi:https://doi.org/10.5194/bg-17-2875-2020, 2020b.

Lilover, M.-J., Lips, U., Laanearu, J. and Liljebladh, B.: Flow regime in the Irbe Strait, Aquat. Sci., 60, 253–265, 1998.

Lips, U., Lilover, M.-J., Raudsepp, U. and Talpsepp, L.: Water renewal processes and related hydrographic structures in the Gulf of Riga, in Est. Mar. Inst. Rep. Ser., edited by A. Toompuu and J. Elken, pp. 1–34., 1995.

Lips, U., Zhurbas, V., Skudra, M. and Väli, G.: A numerical study of circulation in the Gulf of Riga, Baltic Sea. Part I: Whole-basin gyres and mean currents, Cont. Shelf Res., 112, 1–13, 2016.

Lips, U., Laanemets, J., Lips, I., Liblik, T., Suhhova, I. and Suursaar, Ü.: Wind-driven residual circulation and related oxygen and nutrient dynamics in the Gulf of Finland (Baltic Sea) in winter, Estuar. Coast. Shelf Sci., 195, 4–15, 2017.

Lukkari, K., Leivuori, M., Vallius, H. and Kotilainen, A.: The chemical character and burial of phosphorus in shallow coastal sediments in the northeastern Baltic Sea, Biogeochemistry, 94, 141–162, doi:10.1007/s10533-009-9315-y, 2009.

~~Mack, L., Attila, J., Aylagas, E., Beermann, A., Borja, A., Hering, D., Kahlert, M., Leese, F., Lenz, R., Lehtiniemi, M., Liess, A., Lips, U., Mattila, O. P., Meissner, K., Pyhälahti, T., Setälä, O., Strehse, J. S., Uusitalo, L., Willstrand Wranne, A. and Birk, S.: A Synthesis of Marine Monitoring Methods With the Potential to Enhance the Status Assessment of the Baltic Sea, Front. Mar. Sci., 7, 823, doi:10.3389/fmars.2020.552047, 2020.~~

~~Mäkinen, J. and Saaranen, V.: Determination of post-glacial land uplift from the three precise levellings in Finland, J. Geod., 72, 516–529, 1998.~~

Matthäus, W. and Franck, H.: Characteristics of major Baltic inflows—a statistical analysis, Cont. Shelf Res., 12(12), 1375–1400, doi:doi:10.1016/0278-4343(92)90060-W, 1992.

Meier, H. E. M. and Saraiva, S.: Projected Oceanographical Changes in the Baltic Sea until 2100, , doi:10.1093/acrefore/9780190228620.013.699, 2020.

Meier, H. E. M., Andersson, H. C., Eilola, K., Gustafsson, B. G., Kuznetsov, I., Müller-Karulis, B., Neumann, T. and Savchuk, O. P.: Hypoxia in future climates: A model ensemble study for the Baltic Sea, Geophys. Res. Lett., 38(24), doi:https://doi.org/10.1029/2011GL049929, 2011.

Meier, H. E. M., Väli, G., Naumann, M., Eilola, K. and Frauen, C.: Recently Accelerated Oxygen Consumption Rates Amplify Deoxygenation in the Baltic Sea, J. Geophys. Res. Ocean., 123(5), 3227–3240, doi:https://doi.org/10.1029/2017JC013686, 2018.

Murphy, R. R., Kemp, W. M. and Ball, W. P.: Long-Term Trends in Chesapeake Bay Seasonal Hypoxia, Stratification, and Nutrient Loading, Estuaries and Coasts, 34, 1293–1309, doi:10.1007/s12237-011-9413-7, 2011.

Ojaveer, E., Ed.: Ecosystem of the Gulf of Riga between 1920 and 1990, Estonian Academy Publishers, Tallinn., 1995.

Olli, K. and Heiskanen, A.-S.: Seasonal stages of phytoplankton community structure and sinking loss in the Gulf of Riga, J. Mar. Syst., 23(1), 165–184, doi:https://doi.org/10.1016/S0924-7963(99)00056-1, 1999.

Omstedt, A., Meuller, L. and Nyberg, L.: Interannual, Seasonal and Regional Variations of Precipitation and Evaporation over the Baltic Sea, Ambio, 26(8), 484–492, 1997.

Petrov, V.: Water balance and water exchange between the Gulf of Riga and the Baltic Proper, Sb. Rab. Rizhskoj GO, 18, 20–40, 1979.

Pitkänen, H., Lehtoranta, J. and Räike, A.: Internal Nutrient Fluxes Counteract Decreases in External Load: The Case of the Estuarial Eastern Gulf of Finland, Baltic Sea, AMBIO A J. Hum. Environ., 30(4), 195–201, doi:10.1579/0044-7447-30.4.195, 2001.

Powilleit, M. and Kube, J.: Effects of severe oxygen depletion on macrobenthos in the Pomeranian Bay (southern Baltic Sea): a case study in a shallow, sublittoral habitat characterised by low species richness, J. Sea Reasearch, 42, 221–234, 1999.

Purina, I., Labucis, A., Barda, I., Jurgensone, I. and Aigars, J.: Primary productivity in the Gulf of Riga (Baltic Sea) in relation to phytoplankton species and nutrient variability, Oceanologia, 60(4), 544–552, doi:https://doi.org/10.1016/j.oceano.2018.04.005, 2018.

Puttonen, I., Mattila, J., Jonsson, P., Karlsson, O. M., Kohonen, T., Kotilainen, A., Lukkari, K., Malmaeus, J. M. and Rydin, E.: Distribution and estimated release of sediment phosphorus in the northern Baltic Sea archipelagos, Estuar. Coast. Shelf Sci., 145, 9–21, doi:10.1016/j.ecss.2014.04.010, 2014.

Puttonen, I., Kohonen, T. and Mattila, J.: Factors controlling phosphorus release from sediments in coastal archipelago areas, Mar. Pollut. Bull., doi:10.1016/j.marpolbul.2016.04.059, 2016.

Raudsepp, U. and Elken, J.: Application of the GFDL circulation model for the Gulf of Riga. In: Toompuu, A., Elken, J. (Eds.), Est. Mar. Inst. Rep. Ser., 1, 143–176, 1995.

~~Raudsepp, U. and Kõuts, T.: Observations of near-botoom currents in the Gulf of Riga, Baltic Sea, Aquat. Sci., 63, 385–405, 2001.~~

Ruosteenoja, K., Vihma, T. and Venäläinen, A.: Projected Changes in European and North Atlantic Seasonal Wind Climate Derived from CMIP5 Simulations, J. Clim., 32(19), 6467–6490, doi:10.1175/JCLI-D-19-0023.1, 2019.

Saraiva, S., Markus Meier, H. E., Andersson, H., Höglund, A., Dieterich, C., Gröger, M., Hordoir, R. and Eilola, K.: Baltic Sea ecosystem response to various nutrient load scenarios in present and future climates, Clim. Dyn., 52(5), 3369–3387, doi:10.1007/s00382-018-4330-0, 2019a.

Saraiva, S., Meier, H. E. M., Andersson, H., Höglund, A., Dieterich, C., Gröger, M., Hordoir, R. and Eilola, K.: Uncertainties in Projections of the Baltic Sea Ecosystem Driven by an Ensemble of Global Climate Models, Front. Earth Sci., 6, 244, doi:10.3389/feart.2018.00244, 2019b.

Savchuk, O. P.: Large-Scale Nutrient Dynamics in the Baltic Sea, 1970–2016, Front. Mar. Sci., 5, doi:10.3389/fmars.2018.00095, 2018.

Schinke, H. and Matthäus, W.: On the causes of major Baltic inflows —an analysis of long time series, Cont. Shelf Res., 18(1), 67–97, doi:10.1016/S0278-4343(97)00071-X, 1998.

Schlitzer, R.: Ocean Data View, 2019.

Schmale, O., Krause, S., Holtermann, P., Power Guerra, N. C. and Umlauf, L.: Dense bottom gravity currents and their impact on pelagic methanotrophy at oxic/anoxic transition zones, Geophys. Res. Lett., 43(10), 5225–5232, doi:10.1002/2016GL069032, 2016.

Schmidt, B., Wodzinowski, T. and Bulczak, A. I.: Long-term variability of near-bottom oxygen, temperature, and salinity in the Southern Baltic, J. Mar. Syst., 213, 103462, doi:https://doi.org/10.1016/j.jmarsys.2020.103462, 2021.

Séférian, R., Baek, S., Boucher, O., Dufresne, J. L., Decharme, B., Saint-Martin, D. and Roehrig, R.: An interactive ocean surface albedo scheme: Formulation and evaluation in two atmospheric models, Geosci. Model Dev. Discuss., 1–38,

doi:https://doi.org/10.5194/gmd-2017-111, 2017.

Simpson, J. H., Brown, J., Matthews, J. and Allen, G.: Tidal Straining, Density Currents, and Stirring in the Control of Estuarine Stratification, Estuaries, 13(2), 125–132, doi:10.2307/1351581, 1990.

Skudra, M. and Lips, U.: Characteristics and inter-annual changes in temperature, salinity and density distribution in the Gulf of Riga, Oceanologia, 59, 37–48, 2017.

Soosaar, E., Maljutenko, I., Raudsepp, U. and Elken, J.: An investigation of anticyclonic circulation in the southern Gulf of Riga during the spring period, Cont. Shelf Res., 78, 75–84, doi:https://doi.org/10.1016/j.csr.2014.02.009, 2014.

Spilling, K., Olli, K., Lehtoranta, J., Kremp, A., Tedesco, L., Tamelander, T., Klais, R., Peltonen, H. and Tamminen, T.: Shifting Diatom—Dinoflagellate Dominance During Spring Bloom in the Baltic Sea and its Potential Effects on Biogeochemical Cycling, Front. Mar. Sci., 5, doi:10.3389/fmars.2018.00327, 2018.

Stiebrins, O. and Väling, P.: Bottom sediments of the Gulf of Riga, Geol. Surv. Latv. Riga, 4, 1996.

Stipa, T., Tamminen, T. and Seppälä, J.: On the creation and maintenance of stratification in the Gulf of Riga, J. Mar. Syst., 23, 27–49, 1999.

Stoicescu, S.-T., Lips, U. and Liblik, T.: Assessment of Eutrophication Status Based on Sub-Surface Oxygen Conditions in the Gulf of Finland (Baltic Sea), Front. Mar. Sci., 6, 54, doi:10.3389/fmars.2019.00054, 2019.

Stonevičius, E., Rimkus, E., Štaras, A., Kažys, J. and Valiuškevičius, G.: Climate change impact on the Nemunas River basin hydrology in the 21st century, Boreal Environ. Res., 22, 49–65, 2017.

Ukrainskii, V. V. and Popov, Y. I.: Climatic and hydrophysical conditions of the development of hypoxia in waters of the northwest shelf of the Black Sea, Phys. Oceanogr., 19(3), 140–150, doi:0928-5105/09/1903–0140, 2009.

Virtanen, E. A., Norkko, A., Nyström Sandman, A. and Viitasalo, M.: Identifying areas prone to coastal hypoxia -- the role of topography, Biogeosciences, 16(16), 3183–3195, doi:10.5194/bg-16-3183-2019, 2019.

Walve, J., Sandberg, M., Larsson, U. and Lännergren, C.: A Baltic Sea estuary as a phosphorus source and sink after drastic load reduction: seasonal and long-term mass balances for the Stockholm inner archipelago for 1968–2015, Biogeosciences, 15, 3003–3025, doi:10.5194/bg-15-3003-2018, 2018.

Wasmund, N., Nausch, G., Gerth, M., Busch, S., Burmeister, C., Hansen, R. and Sadkowiak, B.: Extension of the growing season of phytoplankton in the western Baltic Sea in response to climate change , Mar. Ecol. Prog. Ser., 622, 1–16, 2019.

Wu, J.: Wind-stress coefficients over sea surface from breeze to hurricane, J. Geophys. Res. Ocean., 87(C12), 9704–9706, doi:https://doi.org/10.1029/JC087iC12p09704, 1982.

Yurkovskis, A.: Long-term land-based and internal forcing of the nutrient state of the Gulf of Riga (Baltic Sea), J. Mar. Syst., 50, 181–197, doi:10.1016/j.jmarsys.2004.01.004, 2004.

Yurkovskis, A., Wulff, F., Rahm, L., Andruzaitis, A. and Rodriguez-Medina, M.: A Nutrient Budget of the Gulf of Riga; Baltic Sea, Estuar. Coast. Shelf Sci., 37(2), 113–127, doi:https://doi.org/10.1006/ecss.1993.1046, 1993.

Zhang, J., Gilbert, D., Gooday, A. J., Levin, L., Naqvi, S. W. A., Middelburg, J. J., Scranton, M., Ekau, W., Peña, A., Dewitte, B., Oguz, T., Monteiro, P. M. S., Urban, E., Rabalais, N. N., Ittekkot, V., Kemp, W. M., Ulloa, O., Elmgren, R., Escobar-

Briones, E. and der Plas, A. K.: Natural and human-induced hypoxia and consequences for coastal areas: synthesis and future development, Biogeosciences, 7(5), 1443–1467, doi:10.5194/bg-7-1443-2010, 2010.

Page 43: [1] Formatted	Stella-Theresa Stoicescu	1/24/2022 10:01:00 PM

English (United States)

Page 43: [1] Formatted	Stella-Theresa Stoicescu	1/24/2022 10:01:00 PM

English (United States)

Page 43: [2] Formatted	Stella-Theresa Stoicescu	1/24/2022 10:01:00 PM

Font: 9 pt, English (United States)

Page 43: [2] Formatted	Stella-Theresa Stoicescu	1/24/2022 10:01:00 PM

Font: 9 pt, English (United States)

Page 43: [2] Formatted	Stella-Theresa Stoicescu	1/24/2022 10:01:00 PM

Font: 9 pt, English (United States)

Page 43: [2] Formatted	Stella-Theresa Stoicescu	1/24/2022 10:01:00 PM

Font: 9 pt, English (United States)

Page 43: [2] Formatted	Stella-Theresa Stoicescu	1/24/2022 10:01:00 PM

Font: 9 pt, English (United States)

Page 43: [3] Formatted	Stella-Theresa Stoicescu	1/24/2022 10:01:00 PM

Font: 9 pt, English (United States)

Page 43: [3] Formatted	Stella-Theresa Stoicescu	1/24/2022 10:01:00 PM

Font: 9 pt, English (United States)

Page 43: [3] Formatted	Stella-Theresa Stoicescu	1/24/2022 10:01:00 PM

Font: 9 pt, English (United States)

Page 43: [3] Formatted	Stella-Theresa Stoicescu	1/24/2022 10:01:00 PM

Font: 9 pt, English (United States)

Page 43: [3] Formatted	Stella-Theresa Stoicescu	1/24/2022 10:01:00 PM

Font: 9 pt, English (United States)

Page 43: [4] Formatted	Stella-Theresa Stoicescu	1/24/2022 10:01:00 PM

Font: 9 pt, English (United States)

Page 43: [4] Formatted	Stella-Theresa Stoicescu	1/24/2022 10:01:00 PM

Font: 9 pt, English (United States)

Page 43: [4] Formatted	Stella-Theresa Stoicescu	1/24/2022 10:01:00 PM

Font: 9 pt, English (United States)

Page 43: [4] Formatted	Stella-Theresa Stoicescu	1/24/2022 10:01:00 PM

Font: 9 pt, English (United States)

Page 43: [4] Formatted **Stella-Theresa Stoicescu** **1/24/2022 10:01:00 PM**

Font: 9 pt, English (United States)

Page 43: [4] Formatted **Stella-Theresa Stoicescu** **1/24/2022 10:01:00 PM**

Font: 9 pt, English (United States)

Page 43: [4] Formatted **Stella-Theresa Stoicescu** **1/24/2022 10:01:00 PM**

Font: 9 pt, English (United States)

Page 43: [4] Formatted **Stella-Theresa Stoicescu** **1/24/2022 10:01:00 PM**

Font: 9 pt, English (United States)

Page 43: [5] Formatted **Stella-Theresa Stoicescu** **1/24/2022 10:01:00 PM**

English (United States)

Page 43: [5] Formatted **Stella-Theresa Stoicescu** **1/24/2022 10:01:00 PM**

English (United States)

Page 43: [6] Formatted **Stella-Theresa Stoicescu** **1/24/2022 10:01:00 PM**

English (United States)

Page 43: [6] Formatted **Stella-Theresa Stoicescu** **1/24/2022 10:01:00 PM**

English (United States)

Page 43: [7] Formatted **Stella-Theresa Stoicescu** **1/24/2022 10:01:00 PM**

English (United States)

Page 43: [7] Formatted **Stella-Theresa Stoicescu** **1/24/2022 10:01:00 PM**

English (United States)

Page 43: [8] Formatted **Stella-Theresa Stoicescu** **1/24/2022 10:01:00 PM**

Font: 9 pt, English (United States)

Page 43: [8] Formatted **Stella-Theresa Stoicescu** **1/24/2022 10:01:00 PM**

Font: 9 pt, English (United States)

Page 43: [8] Formatted **Stella-Theresa Stoicescu** **1/24/2022 10:01:00 PM**

Font: 9 pt, English (United States)

Page 43: [9] Formatted **Stella-Theresa Stoicescu** **1/24/2022 10:01:00 PM**

English (United States)

Page 43: [9] Formatted **Stella-Theresa Stoicescu** **1/24/2022 10:01:00 PM**

English (United States)